

Geology and regional significance of the Sarnoo Hills, eastern rift margin of the Barmer Basin, NW India

Andrew J. Bladon,^{*} Stuart D. Burley,^{*,†} Stuart M. Clarke^{*} and Hazel Beaumont^{*}

^{*}Basin Dynamics Research Group, Keele University, Keele, UK

[†]Cairn India Limited, Gurgaon, India

ABSTRACT

The Barmer Basin is a poorly understood rift basin in Rajasthan, northwest India. Exposures in the Sarnoo Hills, situated along the central eastern rift margin of the Barmer Basin, reveal a sedimentary succession that accumulated prior to the main Barmer Basin rift event, and a rift-oblique fault network that displays unusual geometries and characteristics. Here, we present a comprehensive study of Lower Cretaceous sedimentology on the basin margin, along with a detailed investigation of rift-oblique faults that are exposed nowhere else in the region and provide critical insights into Barmer Basin evolution. Lower Cretaceous sediments were deposited within a rapidly subsiding alluvial plain fluvial system. Subsequent to deposition, the evolving Sarnoo Hills fault network was affected by structural inheritance during an early, previously unrecognised, rift-oblique extensional event attributed to transtension between India and Madagascar, and formed a juvenile fault network within the immediate rift-margin footwall. Ghaggar-Hakra Formation deposition may have been triggered by early rifting which tectonically destabilised the Marwar Craton prior to the main northeast–southwest Barmer Basin rift event. The identification of early rifting in the Barmer Basin demonstrates that regional extension and the associated rift systems were established throughout northwest India prior to the main phase of Deccan eruptions. Inheritance of early oblique fault systems within the evolving Barmer Basin provides a robust explanation for poorly understood structural complications interpreted in the subsurface throughout the rift. Critically, the presence of syn-rift sedimentary successions within older oblique rift systems obscured beneath the present-day Barmer Basin has significant implications for hydrocarbon exploration.

INTRODUCTION

Despite being a significant structure within the West Indian Rift System (Fig. 1a), and an important hydrocarbon province (Dolson et al., 2015), the structural geology and evolution of the Barmer Basin rift remains relatively poorly understood. The current understanding of rift evolution is based predominantly upon subsurface data sets, where an abundance of complex structures and rift-oblique faults are variably imaged on seismic data throughout the rift (Bladon et al., 2015; Fig. 1b). However, the origin of these structures remains elusive, and limited exposure of the structure and stratigraphy of the rift at outcrop has restricted outcrop-based studies. This work characterises a rift-oblique fault network that is apparent nowhere else in the region, and is exposed on the eastern rift margin of the Barmer Basin, in the Sarnoo Hills. Detailed sedimentological and structural analyses are used to clarify the origin of similar rift-oblique faults imaged in the Barmer Basin subsurface, and subsequently to place the findings within the wider context of northwest India. Sediments were deposited in a maturing fluvial system within a rapidly subsiding continental alluvial plain environment. The exposed rift-oblique fault network was affected by pre-existing structures within the crust (structural inheritance) during a previously unrecognised northwest–southeast extensional event. Importantly, the sedimentary succession accumulated prior to the main Barmer Basin rifting event. Deposition may have been triggered by early rift-oblique extension. Combined, the findings of the sedimentological and structural analyses provide insights into the early-stage structural evolution of the Barmer Basin, and present critical data representing regional tectonic processes hitherto unrecognised. Subsequently, an improved understanding of Barmer Basin rift evolution is presented, alongside a more robust explanation for the poorly understood and atypical rift-oblique faults interpreted on subsurface data throughout the rift. Our findings support the inference that extension throughout northwest India was long-lived and well-established prior to the Cretaceous–Paleogene boundary, and may indicate hidden potential for hydrocarbon exploration beneath the present-day Barmer Basin.

GEOLOGICAL BACKGROUND

Basins of northwest India The rifted north-western margin of India (Fig. 1), active since the early Mesozoic, remains poorly understood despite many hydrocarbon discoveries (Biswas, 1982; Gombos et al., 1995; Compton, 2009; Dolson et al., 2015). Onshore rift basins within the West Indian Rift System include the Kachchh (Kutch), Cambay, and Narmada basins. The Barmer Basin is the most northerly rift within the West Indian Rift System (Fig. 1), and is a long, narrow and deep (200 km, <40 km, & ≤ 6 km respectively), late Cretaceous to mid-Eocene, low-strain ($1.2 \leq b \leq 1.5$), failed continental rift that is linked with the Cambay Basin to the south via the poorly defined Sanchor sub-Basin (Compton, 2009; Dolson et al., 2015). Together, the Barmer and Cambay basins form a north–northwest-trending rift system that extends some 600 km into the Indian continent. To the north of the Barmer Basin, the Jaisalmer Basin forms the eastern slopes of the larger Indus Basin (Singh, 2006, 2007). The Barmer and Jaisalmer basins are separated by a basement structural high, the Devikot High (Fig. 1a). Extension within the West Indian Rift System may have begun as early as the Triassic Period in the Kachchh Basin (Biswas, 1982, 1987). However, significant basin-wide deposition did not occur in the Kachchh Basin until the Jurassic Period (Jhurio/Kaladongar Formation; Krishna, 1987; F€urisch & Pandey, 2003; Pandey et al., 2009). Adjacent to the Kachchh Basin, sub-Deccan strata within the Cambay Basin are poorly imaged and largely unknown in the subsurface (Rohrman, 2007). Based upon surface exposures, Mesozoic sedimentation within the Cambay rift is thought to have occurred in shallow marine, brackish and deltaic environments on an occasionally emergent platform (Raju, 1968; Chowdhary, 1975). To the east of the Cambay Basin, subsidence and deposition within the Narmada Basin began during the Lower Cretaceous. Deposition of the continental Nimar Sandstone occurred prior to a marine transgression throughout the Narmada rift, until eruption of the Deccan Traps (Akhtar & Ahmad, 1991; Khosla et al., 2003; Jaitly & Ajane, 2013). The preservation of Mesozoic deposits throughout the West Indian Rift System alludes to established Mesozoic rifting throughout northwest India that pre-dated the main phase of Deccan eruptions. In the Jaisalmer Basin (Fig. 1a), deposition of the fluvio- deltaic Lathi Formation (≤ 500 m thick) during the Jurassic Period preceded marine deposition that endured until the Upper Cretaceous (Torsvik et al., 2005; Singh, 2006; Pandey et al., 2012; Rai et al., 2013). However, continental deposits that are Jurassic in age occur at outcrop within the Jaisalmer Basin, indicating that marine deposition was intermittent. During the Cretaceous, therefore, the south-western periphery of the Marwar Craton separated a series of marine-embayed rifts to the south (Kachchh, Cambay and Narmada basins), from a shallow-marine passive margin shelf to the north (Jaisalmer Basin). It is across this 300 km wide area that the Barmer Basin rift subsequently developed. The majority of subsidence along the West Indian Rift System occurred near to the Cretaceous–Paleogene boundary and was contemporaneous with rifting of the Seychelles microcontinent from northwest India and the main phase of Deccan eruptions (65 Ma; Chenet et al., 2007). Although Seychelles rifting and the Deccan extrusions were closely related (Collier et al., 2008), the cause of extension throughout northwest India at this time is speculative. Extension is commonly assumed to have resulted from the impact of the Réunion mantle plume beneath the Indian peninsular (e.g. Morgan, 1971; Plummer & Belle, 1995; Simonetti et al., 1995). However, alternative views suggest that Seychelles rifting resulted from external plate boundary forces (Sheth, 2005a; Sharma, 2007; Collier et al., 2008; Bladon et al., 2015), and many aspects of the Deccan geology have been shown to be inconsistent with plume activity, being more typical of deep-seated rifting (Sheth, 2005a,b, 2007; Sharma, 2007). In addition, the thick sequence of late Cretaceous to Eocene sediments (>6 km) in the Barmer Basin is counter to the impingement of a mantle plume beneath northwest India near to the Cretaceous–Paleogene boundary, despite the presence of multiple rift-related unconformities within the rift.

The Barmer Basin

Until recently, the extent, structure and geology of the Barmer Basin were poorly constrained, and only as subsurface data became available over the last decade has an appreciation of the scale and significance of the rift been achieved (Dolson et al., 2015). Rift-basement rocks in the Barmer Basin comprise the Precambrian Malani Igneous Suite (c.f. Pareek, 1981; Fig. 2). Unconformably overlying the Malani Igneous Suite, exposures of the Jurassic Lathi Formation in the north Barmer Basin (Fatehgarh Ridge), and the Lower Cretaceous Ghaggar-Hakra Formation along the central eastern rift

margin (Sarnoo Hills; Sisodia & Singh, 2000; Dolson et al., 2015), indicate that Mesozoic deposition occurred in the Barmer region prior to the main Barmer Basin rift event. The syn-rift sedimentary succession in the Barmer Basin is predominantly Paleocene to Eocene in age, and comprises a progression from fluvial through shallow lacustrine to deep lacustrine deposition, prior to post-rift infilling of the Barmer Basin lake with low energy fluvial and floodplain sediments (Dolson et al., 2015). The main phase of extension within the Barmer Basin *sensu stricto* occurred between the late Cretaceous (Maastrichtian) and mid-Eocene (Lutetian). However, exposure of two different and distinct extensional structural regimes on opposing rift margins, combined with temporally variable subsurface depocentre orientations within early syn-rift deposits, indicated that evolution of the Barmer Basin resulted from two non-coaxial extensional events (Bladon et al., 2015). Early rift-oblique (NW–SE) extension within the Barmer Basin may be a manifestation of transtension between the Greater Indian and Madagascan continents during the separation of east and west Gondwana (Bladon et al., 2015). Recently, large-scale uplift in the north of the basin (>1 km) likely resulted from the collision of India with Eurasia, with the present-day peneplanation of the northern Barmer Basin being the current expression of this uplift (Dolson et al., 2015). In contrast to the northern part of the Barmer Basin, the southern part of the basin has undergone continuous subsidence since the end of extension in the mid Eocene, which, when coupled with uplift in the north, has resulted in a gentle tilting of the basin to the southeast.

The Sarnoo Hills

Situated along the central eastern rift margin of the Barmer Basin (Fig. 1), the Sarnoo Hills are a prominent series of northeast-trending ridges in the vicinity of the village of Sarnoo (alternatively spelt 'Sarnu' or 'Saranu'). Interbedded sands and silts of the Ghaggar-Hakra Formation are exposed overlying mafic crystalline rocks (Sisodia & Singh, 2000). Previously part of the Sarnu[sic] Formation (also termed the Sarnu Sandstone), the Ghaggar-Hakra Formation was assigned a poorly constrained Middle Jurassic to Lower Cretaceous age based on plant fossils recovered from the Sarnoo Hills (Baksi & Naskar, 1981). Initial studies by the authors (Bladon et al., 2015) indicated that dominant faults are southwest-striking and define southeast-dipping rotated normal fault blocks compartmentalised by oblique faulting. A rift-oblique (NW–SE) extension direction and control of pre-existing structures was postulated. Exposure in the Sarnoo area is dominated by rhyolite and rhyolitic tuff of the Precambrian Malani Igneous Suite (Roy & Jakhar, 2002) that forms the rift basement of the Barmer Basin. Alkali olivine basalt, hawaiites, trachyandesite, and trachyte of poorly constrained age immediately overlie the Malani Igneous Suite (Roy & Jakhar, 2002). An Aptian age has been suggested for these mildly alkaline igneous rocks (120 Ma), with a genesis associated with regional extension arising from Gondwana fragmentation (Sharma, 2007). An intrusive origin has also been postulated (Sisodia & Singh, 2000). In-turn, this suite of mafic igneous rocks is overlain by the Middle Jurassic to Lower Cretaceous sedimentary succession of the Ghaggar-Hakra Formation (Baksi & Naskar, 1981; Sisodia & Singh, 2000; Roy & Jakhar, 2002). Subsequent to deposition of the Ghaggar-Hakra Formation, a diverse suite of acid, intermediate and alkaline plug-like bodies (Sarnu[sic]-Dandali Suite), associated with an early phase of Deccan igneous activity (68.57 ± 0.08 Ma; Basu et al., 1993), were emplaced and are exposed throughout the Sarnoo area (Basu et al., 1993; Simonetti et al., 1995, 1998; Roy & Jakhar, 2002; Roy, 2003; Sen et al., 2012).

METHODOLOGY

High resolution geological mapping was conducted throughout the Sarnoo Hills in conjunction with interpretation of satellite imagery. Where available, extensional fracture plane, fault plane and fault-plane slickenline lineation data were recorded. Logging of the sedimentary succession accompanied geological mapping, as well as architectural, textural and petrographical (thin section) descriptions of each mapping unit. Using the lithological contacts and faults mapped at outcrop, structural data and general field observations, a three-dimensional virtual structural model of the outcrop was constructed from 20 northwest–southeast orientated (305°–125°) two-dimensional cross-sections. Surface data were projected onto the Digital Elevation Model, faults were assumed to dip at a constant 61°, and the thicknesses of stratigraphical units were varied according to field observations. During construction and upon completion, the model was quality controlled and visually inspected to ensure its

compatibility with the outcrop. Observations made at outcrop were used to make sensible interpretations in areas of no exposure. Subsequently, the virtual outcrop model was used to construct fault displacement-length profiles for key faults within the Sarnoo Hills fault network.

THE SARNOO HILLS

Stratigraphy

The mafic crystalline rocks at the base of the succession comprise predominantly microcrystalline plagioclase laths and sphene, with some interstitial glass (Fig. 3a). In some samples, irregular chlorite-filled enclaves are observed (Fig. 3a). Occasionally, a heavily altered, poorly consolidated, light green crystalline unit appears interbedded within the lowermost Ghaggar-Hakra Formation (Fig. 4a). However, a superficially similar unit often displays cross-cutting relationships within the sedimentary succession (Fig. 4b). Overlying the crystalline rocks, the Ghaggar-Hakra Formation (Fig. 2) comprises three arenaceous successions separated by thick mudstone and siltstone packages (≤ 30 m) that contain thin arenite interbeds (≤ 0.5 m; Fig. 5). The mudstone and siltstone packages are generally red and horizontally laminated, but contain both symmetrically and asymmetrically ripple cross-laminated units, mottled and rooted horizons, and rare soft-sediment deformation. The lowermost lithic arenite succession, the Darjaniyon-ki Dhani Sandstone (dar; Fig. 5), comprises a poorly sorted, clast-supported, coarse- to granule-grade litharenite containing polymictic, angular clasts (Fig. 3c). Crude planar and trough cross-bedded sets are 0.5–1 m thick, and show strongly erosive bases, crude channel geometries, and are generally normally graded. The middle arenite succession, the Sarnoo Sandstone (sar; Fig. 5), is a well-sorted, clast-supported and fine- to medium-grained quartz arenite, with well-rounded, monomictic quartz clasts (Fig. 3d). Coarse to very coarse, occasionally granule-grade clasts occur in lags at the base of channel geometries, alongside abundant siltstone rip-up clasts. Beds are 0.5–2 m thick and generally planar cross-bedded or horizontally bedded. However, trough cross-bedding and erosive bases are occasionally evident. Thick beds (≤ 2 m) of fine- to very fine-grained extensively rippled and ripple cross-laminated units are also observed. The uppermost quartz arenite succession, the Nosar Sandstone (nos; Fig. 5) that caps the prominent hills, is moderately sorted, clast-supported, coarse- to very coarse-grained, and contains abundant granules and pebbles, with subangular to sub-rounded, predominantly quartzitic clasts (Fig. 3e). Cross-bedded sets are 0.5–3 m thick, highly erosive with abundant siltstone rip-up clasts, and are both planar and trough cross-bedded. Foresets are commonly normally graded from pebble- to coarse-sand grade, and authigenic illite and kaolinite cement gives the sandstone a striking white colour. Although no upper contact is preserved, the Nosar Sandstone is at least 30 m thick in some exposures. Nowhere in the Sarnoo Hills do synsedimentary growth successions occur, or do the sedimentary units show thickness variations across faults.

Structure

Three structural trends are evident on satellite imagery: (i) northeast–southwest; (ii) east–west; and (iii) eastnortheast–west-southwest, as well as three prominent outcrop-dissecting topographical depressions (Fig. 6). Field observations confirm that southwest-striking (210° – 220°), northwest-dipping, ridge-parallel faults are dominant, defining ridge-parallel valleys in the north and south of the exposure. Southwest-striking faults accommodate large displacements (≤ 80 m) on discrete slip-surfaces that form narrow (< 5 m) damage zones (Fig. 7a). West-striking (270° – 280°), north-dipping faults accommodate less displacement (≤ 25 m; Fig. 7b, c), and correspond to the outcrop-dissecting topographical depressions evident on satellite imagery (Fig. 6). Although discrete west-striking faults do not occur everywhere along the outcrop-dissecting depressions, these topographical features are characterised by a broad zone of concentrated, low-strain deformation features (e.g. fractures, small-offset faults) that accommodate negligible aggregate displacement. Combined, west- and southwest-striking faults form a zig-zag fault network with west–southwest-striking (240° – 250°) faults accommodating comparatively minor deformation within faulted blocks (Fig. 8).

On average, the dip of the strata is 15° to the southeast (126° dip-azimuth), with north–northwest-trending fractures, and east-trending faults most prevalent (Fig. 9). Although variable, the average dip

of the faults is 61° ($n = 337$; standard deviation = 15°). Rift-parallel fractures were commonly observed oblique to large fault cores (Fig. 10c). Within the competent sandstone successions, fault zones typically comprise thick packages of faultgouge (≤ 1 m), with brittle damage zones being variably present (Fig. 10a–c). Occasionally, gouge thickness is disproportionately large for observed fault displacement (e.g. 1 m wide for 0.9 m offset). In contrast, within the thick mudstone and siltstone packages faults are obscure, and deformation occurs on discrete slip-planes. Excellent exposure of in-plane fault kinematic (slickenline) data (Fig. 10d–f) shows predominantly normalsense, dip-slip movement to the northwest, with a mean resultant slip direction of 308° (Fig. 11a). Fault-plane slickenlines occur almost exclusively in one consistent orientation (single-generation; Fig. 10d–f) rather than as several, cross-cutting slickenline sets (multiple-generation). Insights into the kinematics of the fault network were attained by categorising slip data by fault strike (Fig. 11b, c). Both southwest- and west-striking faults accommodated unimodal slip to the northwest (313° and 326° respectively); however, a 013° disparity exists between average slickenline trends (Fig. 11). Fault slip on southwest-striking faults is predominantly normal slip (i.e. slickenline pitch $\sim 90^\circ$), with average pitch measurements of 87° (3° component of sinistral-oblique slip), whereas fault slip on west-striking faults displays a significant component (15°) of sinistral-oblique slip (average pitch = 75° ; Fig. 12). Little evidence of fault reactivation is observed in the Sarnoo Hills, despite evidence supporting multiple non-coaxial rift events in the Barmer Basin (Bladon et al., 2015), the recent collision between India and Eurasia, and the associated inversion recorded elsewhere in the Barmer Basin (Dolson et al., 2015).

Outcropmodel

The fault network simulated by the three-dimensional model of the outcrop (Fig. 13) satisfactorily replicates the fault network exposed at outcrop (Fig. 8). Fault displacement-length profiles were generated using the base Nosar Sandstone surface, the most significant and consistent surface exposed (Fig. 14). Although the base Nosar Sandstone surface is erosive (≤ 4 m), it can be used reliably to correlate across faults because deposition pre-dates deformation. In areas where southwest- and west-striking faults interact, fault displacement-length profiles are erratic (Fig. 14). An important feature is the near complete loss of displacement on some sections of southwest-striking faults towards west-striking faults (starred in Fig. 14).

DEPOSITION OF THE GHAGGAR HAKRA FORMATION

The mafic crystalline rock underlying the Ghaggar-Hakra Formation has characteristic basaltic mineralogy in accordance with previous interpretations (Roy & Jakhar, 2002). Within this unit, the irregular chlorite-filled enclaves (Fig. 3a) are interpreted as infilled vesicles, supporting shallow emplacement or sub-aerial extrusion. A distinct lack of evidence for thermal interaction between the basalt and the overlying sediments of the Ghaggar-Hakra Formation (chilled/baked margins) suggests the former is not intrusive and deposition of the latter occurred directly onto the exposed upper surface of the basalt. Although apparently interbedded with the Ghaggar-Hakra Formation in places (Fig. 4a), the heavily altered, light green crystalline unit at the base of the succession is interpreted as intrusive based on the definite cross-cutting relationship displayed with the sedimentary succession (Fig. 4b) and, therefore, is the youngest unit within the exposed succession. The lowermost sandstone succession, the Darjaniyonki Dhani Sandstone (dar; Fig. 15), represents immature, braided fluvial deposition with a high sediment load, in mobile, erosive channels. The middle sandstone succession, the Sarnoo Sandstone (sar; Fig. 15), displays features typical of deposition within a much larger fluvial system, as indicated through stacked channel elements and an increase in the maturity of clasts. Sedimentary logs show facies associations characteristic of waning fluid flow successions, with pebble-lags and siltstone rip-up clasts indicative of channel migration or a seasonally recharged system. Thick, extensively rippled units (0.5–2 m) represent unconfined deposition within sheetfloods. The Sarnoo Sandstone reflects deposition within a mobile, meandering fluvial system. Preservation of stacked accreting channel systems with highly erosive bases, a lack of preserved channel geometries, and siltstone rip-up clasts, suggests deposition of the uppermost sandstone succession, the Nosar Sandstone (nos; Fig. 15) occurred within an active, rapidly migrating fluvial system that was dominantly braided. Although moderately sorted and medium- to

very coarse-grained, the mature clast array may indicate intraformational reworking. The lack of in-situ overbank material and channel geometries suggests that channel migration was rapid, or that sediment input was high relative to subsidence. Overall, the sandstone successions of the Ghaggar-Hakra Formation show deposition within a maturing-upwards, mobile fluvial succession that displays a temporal increase in the size of the system. Relative to the sandstone successions, the intervening mudstones and siltstones occur in unusually thick packages (≤ 30 m) and likely represent the floodplain environment that accompanied the Darjaniyon-ki Dhani and Sarnoo sandstone fluvial systems. Rooted horizons within the siltstone and mudstone packages allude to sub-aerial exposure and the beginning of pedogenesis. However, the high proportion of fine deposits within the sedimentary succession suggests aggradation of the floodplain, possibly due to rapid subsidence and a high sediment supply, which implies a high rate of flooding within the fluvial system. Rapid rates of floodplain aggradation (>0.5 cm year⁻¹) limit soil formation and pedogenic assimilation (Daniels, 2003), and is consistent with the limited evidence for long-term floodplain stabilisation within the exposed sedimentary succession. Deposition of the mudstones and siltstones within ephemeral lakes during long-lived periods of flooding may also account for high proportion of fines within the Sarnoo Hills sedimentary succession. In summary, the sedimentary succession exposed in the Sarnoo Hills represents fluvial deposition within a rapidly subsiding continental alluvial plain system that, at times, had a high sediment supply.

STRUCTURAL EVOLUTION OF THE SARNOO HILLS

The near-exclusive trend of single-generation, normalsense slickenlines towards the northwest, and the southwest- striking orientation of major faults, indicates fault activity during a single phase, or multiple coaxial phases, of northwest–southeast extension. The presence of a dominant north–northwest-trending extensional fracture set (Fig. 9), however, indicates that the Sarnoo Hills underwent a period of northeast–southwest extensional deformation. Fault blocks deformed internally on west– southwest-striking (240° – 250°) subsidiary faults (Fig. 8). A lack of growth faulting and fault-related stratigraphical thickness changes signifies that deformation post-dates deposition. The depth of deformation remains unknown; however, the large component of mode one (pure-shear) opening evident on many faults suggests deformation was shallow. A combination of block-rotations during deformation, and tilting during the recent uplift and subsidence of the northern and southern rift respectively, rotated the strata towards the southeast by an average 15° . The average 15° component of sinistral-oblique slip of west-striking faults exposed in the Sarnoo Hills (Fig. 12) suggests these faults were orientated obliquely to the extension direction. By comparison, the near pure normal slip of southwest-striking faults (average 87° pitch; Fig. 12), and the larger displacement accommodated by these faults, indicates they were orientated approximately perpendicular to the direction of extension. It follows that west-striking faults were influenced by pre-existing, extension-oblique, rift-basement faults, and were incorporated into the evolving extension-perpendicular, southwest- striking fault systems during northwest–southeast extension. The concomitance between west-striking faults and the outcrop-dissecting topographical depressions (Fig. 13) suggests that the depressions are a subtle indicator of a discrete rift-basement fabric at depth. West-striking faults do not occur everywhere along the length of the topographical depressions (Fig. 13) indicating partial, not complete reactivation of the underlying rift-basement fabric. The incorporation of west-striking faults within the evolving southwest-striking fault network indicates that both fault trends were active contemporaneously and underwent a mutual slip. A mutual slip of southwest- and west-striking faults may account for the 013° disparity in average slickenline trends (e.g. Nieto-Samaniego & Alaniz- Alvarez, 1997; Fig. 11). The near complete loss of displacement on some sections of the extension-perpendicular (SW-striking) faults towards the reactivated, extension-oblique (W-striking) fault segments (starred on Fig. 14b, d), indicates that reactivated fault segments restricted the evolution of the extension-perpendicular (SW-striking) fault systems. Similar relationships have been observed experimentally (Bellahsen & Daniel, 2005), and were attributed to the reactivated pre-existing fault acting as a ‘stress barrier’ that inhibited the lateral propagation of the evolving faults due to a perturbed stress field (e.g. Willemse, 1997).

DISCUSSION

Chronology

If the Aptian age proposed for the basalt underlying the Ghaggar-Hakra Formation is credible (120 Ma; Sharma, 2007), deposition cannot have occurred prior to this time. Such an age inference falls within the poorly constrained Middle Jurassic to Lower Cretaceous estimate proposed for the Ghaggar-Hakra Formation previously based on plant fossils (Baksi & Naskar, 1981), and further constrains deposition to the Aptian and Albian. Additional sample dating is required to validate and refine these limits. The intrusions within the sedimentary succession are the youngest unit exposed in the Sarnoo Hills and most likely correspond to the early phase of Deccan igneous activity (68.57–0.08 Ma; Basu et al., 1993) exposed locally as scattered plug-like bodies (Basu et al., 1993; Simonetti et al., 1995, 1998; Roy & Jakhar, 2002; Roy, 2003; Sen et al., 2012). Although poorly constrained, the Aptian to Albian age estimate for the Ghaggar-Hakra Formation, and Maastrichtian age of intrusions, occasionally exposed within existing fault planes, crudely constrains the deformation event exposed in the Sarnoo Hills to have occurred between the Aptian and Maastrichtian.

Northwest–Southeast extension

The description of structures exposed in the Sarnoo Hills provides a detailed account of rift-oblique faults in the Barmer Basin, and further outcrop-based evidence for the previously unrecognised rift-oblique (NW–SE) extensional event that preceded the main, rift-orthogonal (NE–SW) Barmer Basin rift event (e.g. Bladon et al., 2015). Structural activity on southwest-trending, rift-oblique faults throughout the subsurface (c.f. Bladon et al., 2015) substantiates that extension was regional, and that the northwest-extension observed in the Sarnoo Hills was not locally derived from, for example, gravity-induced footwall collapse (e.g. Hesthammer & Fossen, 1999). Incorporation of rift-oblique faults generated during early rift-oblique extension, into the evolving fault systems during the main, rift-orthogonal Barmer Basin rift event (e.g. Bonini et al., 1997; Keep & McClay, 1997; Morley et al., 2007), provides a robust explanation for structural complications and poorly understood rift-oblique faults interpreted in the subsurface throughout the rift (Fig. 1b; Bladon et al., 2015). The speculation that deformation occurred between the Aptian and Maastrichtian is in accordance with an early rift-oblique extensional event in the Barmer Basin related to transtension between the Madagascan and Greater Indian continents (e.g. Bladon et al., 2015), prior to successful separation during the Turonian (88 Ma; Storey et al., 1995). The documentation of mid-Cretaceous extension in the Barmer Basin, linked to external plate boundary forces, indicates that extension throughout northwest India was long-lived, resulted from far-field plate reorganisations, and was established prior to the main phase of Deccan eruptions (~65 Ma).

Ghaggar-Hakra Formation deposition

The initially immature deposits, rapid subsidence and high sediment input interpreted from exposures of the Ghaggar-Hakra Formation in the Sarnoo Hills (Fig. 15), indicate that deposition marked a sudden change to long-lived, stable conditions on the craton interior, as indicated by the significant regional unconformity above Malani Igneous Suite deposits throughout northwest India (Sisodia & Singh, 2000; Dolson et al., 2015). Although the migration of the Indian Peninsular during the Mesozoic (e.g. Torsvik et al., 2005) may have induced important climatic variations throughout northwest India, tectonic destabilisation of the Marwar Craton during early, rift-oblique (NW–SE) extension is favoured as the trigger of Ghaggar-Hakra Formation deposition. Rapid extension-induced subsidence in the Barmer region may have captured established regional drainage systems (Fig. 16), accounting for the high sediment input. We tentatively suggest that the Aravalli Mountains, immediately east and southeast of the Barmer Basin, formed during the Proterozoic (Mamtani et al., 2000; Vijaya Rao et al., 2000), are a probable hinterland for Ghaggar-Hakra Formation deposits. The pre-rift tectono-stratigraphical relationships and lack of syn-kinematic strata exposed in the Sarnoo Hills suggests initial northwest–southeast deformation occurred elsewhere in the Barmer region before migrating into the Sarnoo Hills. Deposition within a developing extensional terrane implies that the Ghaggar-Hakra Formation may exhibit syn-rift tectono-stratigraphical relationships elsewhere in the Barmer region. Critically, the presence of thick fluvial successions within early, southwest-trending (rift-oblique) rift systems that are presently obscured beneath the Barmer Basin has significant potential for hydrocarbon exploration.

The Sarnoo Hills fault network

The involvement of pre-existing structures that are inherent in the crust during extension has been investigated extensively through combined experimental, seismic and outcrop studies (Lezzar et al., 2002; McClay et al., 2002; Younes & McClay, 2002; Morley et al., 2004; Bellahsen & Daniel, 2005; Bellahsen et al., 2006; Henza et al., 2010, 2011; Giba et al., 2012; Chattopadhyay & Chakra, 2013; Reeve et al., 2014; Whipp et al., 2014). However, few detailed studies exist that characterise the effect that structures inherent in the crust can have on an evolving extensional fault network based on outcrop-data alone (e.g. McClay & Khalil, 1998). Pre-existing fabrics within the crust may be reactivated at high angles (60°) to the extension direction (Morley, 1995) and are most prevalent during the earliest stages of extension, at which time strain is accommodated on competing pre-existing and rift-generated faults (Morley et al., 2004). As extension proceeds, extension-perpendicular (extension-ideal) faults become dominant (Lezzar et al., 2002; Bellahsen & Daniel, 2005). Where pre-existing faults interact with evolving fault systems, fault geometries tend not to display that expected from classical and idealised models, but instead often form 'crooked X-shapes' and 'zig-zag' patterns (Morley, 1995). As faults grow and link, such irregularities may become smoothed out or obliterated (Morley, 1995). Even if inactive (or slightly active), pre-existing fabrics may hinder the evolution of rift-generated faults (Bellahsen & Daniel, 2005). As such, pre-existing fabrics are classified as pervasive or discrete based upon their characteristics, and as active or passive based upon their behaviour (Morley, 1999). Active fabrics act as a through-going structure with a unique sense of shear (e.g. a through-going strike-slip zone) and passive fabrics locally influence fault terminations and orientations (Morley, 1999). In the Sarnoo Hills, partial reactivation of the underlying west-striking rift-basement fabric indicates passive behaviour (c.f. Morley, 1999) during northwest–southeast extension. However, where reactivated west-striking fault segments restricted the evolution of southwest-striking faults, the reactivated fault segment acted as a through-going fault with a distinct sense of shear, and locally exhibited active behaviour (Fig. 17).

Characteristics of the Sarnoo Hills fault network, including: (i) the high degree of involvement of reactivated fault segments; (ii) the strong influence that reactivated fault segments had on the evolving extension-ideal (southwest-striking) fault systems and (iii) the prominent zig-zag geometry, indicate that extension-perpendicular faults did not become dominant, nor was the zig-zag geometry 'smoothed out,' as is expected to occur during fault network maturation (Morley, 1999; Lezzar et al., 2002; Bellahsen & Daniel, 2005). Such traits indicate that fault activity occurred during incipient northwest–southeast extension, and the fault network did not mature from the incipient stages of formation. The proximity of the outcrop to a major rift-margin fault, sub-parallel to dominant extension-perpendicular (SW-striking) faults in the Sarnoo Hills (Fig. 13a), indicates that strain became localised onto this fault during northwest–southeast extension, preserving the juvenile Sarnoo Hills fault network in the immediate rift-margin footwall. Due to the lack of development of efficient, throughgoing, southwest-striking faults, the zig-zag nature of the juvenile fault network would have actively hindered sinistral-oblique reactivation of southwest-striking faults during the main northeast–southwest Barmer Basin rift event. However, the complete syn-rift sedimentary succession at the base of the rift-oblique rift-margin fault adjacent to the Sarnoo Hills (Fig. 1d) indicates this fault was active for the duration of rifting. We postulate that the tabular geometry of early stratigraphical intervals at the base of the rift-oblique rift-margin fault (Fig. 1d), and thickness variations towards and across active rift-parallel faults to the north and south of the Sarnoo Hills (Fig. 1c, e) suggest a significant component of oblique slip, and suppressed dip-slip movement, of the former. We speculate that, during northeast–southwest orientated Paleogene extension, sinistral-oblique reactivation of the rift-margin fault would have been favourable to overcoming (obliterating) irregularities in the juvenile Sarnoo Hills fault network inherited from the early rift-oblique (NW–SE) extensional event. Such a hypothesis implies that faults in the Sarnoo Hills remained inactive during the main Barmer Basin rift event accounting for the lack of evidence for oblique reactivation of faults. However, northeast–southwest extension is expressed in the Sarnoo Hills as distributed, low-strain deformation (i.e. extension fractures; Fig. 9, 10c).

CONCLUSIONS

The Ghaggar-Hakra Formation comprises a series of fluvial sandstone successions separated by thick packages of mudstone and siltstone, deposited within a maturing fluvial system. The fault network exposed in the Sarnoo Hills comprises a rift-oblique, zig-zag fault network of southwest and west-striking faults that evolved during northwest–southeast extension. West-striking faults were influenced by pre-existing rift-basement faults and the evolution of extension-perpendicular (SW-striking) faults was restricted by reactivated segments of pre-existing rift-basement (W-striking) faults that exhibited both active and passive behaviour.

Deposition of the Ghaggar-Hakra Formation may have occurred during the Lower Cretaceous, triggered by an early rift-oblique (NW–SE) extensional event that preceded the main, rift-orthogonal (NE–SW) Barmer Basin rift event. Early rifting is suggested to be related to transtension between the Greater Indian and Madagascan continents prior to successful separation, and implies that rifting resulted from far-field plate boundary forces prior to the main phase of Deccan eruptions (65 Ma). Incorporation of rift-oblique faults generated during early rift-oblique (NW–SE) extension into the evolving fault systems during the main Barmer Basin rift event (i.e. two episodes of non-coaxial extension), provides a robust explanation for structural complications and poorly understood rift-oblique faults interpreted in the subsurface throughout the rift. Elsewhere in the Barmer Basin, the Ghaggar-Hakra Formation is most likely present within early rift systems obscured beneath the Paleogene Barmer Basin rift, and exhibit comparable Mesozoic syn-rift tectono-stratigraphical relationships. Such hidden Mesozoic rifts offer significant potential for future hydrocarbon exploration in the Barmer region of Rajasthan.

ACKNOWLEDGEMENTS

Keele University (Acorn Fund) and Cairn India Limited are thanked for funding this research. Cairn India Limited generously provided logistical support and assistance in the field, where the kind assistance of Bhanwar Lal made field work both safe and most enjoyable. Richard Burgess is gratefully acknowledged for his invaluable assistance in the Keele University labs, without which this work would not have been possible. Cynthia Ebinger is thanked as editor, along with Chris Morley and Sverre Planke for constructive reviews. Schlumberger Information Systems kindly provided an academic licence for Petrel TM, which was used to construct the virtual structural model of the outcrop using the corner point gridding workflow, as did Midland Valley for MoveTM, used to produce the cross-sections from which the three-dimensional model was constructed and to depth-convert the interpreted seismic sections. Cairn India Limited kindly provided permission to publish, and colleagues in the Basin Dynamics Research Group at Keele are thanked for helpful discussions during the course of this work.

REFERENCES

- AKHTAR, K. & AHMAD, A.H.M. (1991) Single-cycle cratonic quartzarenites produced by tropical weathering: the Nimar sandstone (Lower Cretaceous), Narmada basin, India. *Sed. Geol.*, 71, 23–32.
- BAKSI, S.K. & NASKAR, P. (1981) Fossil plants from the Sarnoo Hill formation, Barmer Basin, Rajasthan. *Palaeobotanist*, 27, 107–111.
- BASU, A.R., RENNE, P.R., DASGUPTA, D.K., TEICHMANN, F. & POREDA, R.J. (1993) Early and late alkali igneous pulses and a high-³He plume origin for the Deccan flood basalts. *Science*, 261, 902–906.
- BELLAHSEN, N. & DANIEL, J.M. (2005) Fault reactivation control on normal fault growth: an experimental study. *J. Struct. Geol.*, 27, 769–780.
- BELLAHSEN, N., FOURNIER, M., D'ACREMONT, E., LEROY, S. & DANIEL, J.M. (2006) Fault reactivation and rift-localisation: Northeastern Gulf of Aden margin. *Tectonics*, 25, TC1007,

doi: 10.1029/2004TC001626.

- BISWAS, S.K. (1982) Rift basins in Western Margin of India and their hydrocarbon prospects with special reference to Kutch Basin. *Am. Assoc. Pet. Geol. Bull.*, 66(10), 1497–1513.
- BISWAS, S.K. (1987) Regional tectonic framework, structure and evolution of the western marginal basins of India. *Tectonophysics*, 135, 307–327.
- BLADON, A.J., CLARKE, S.M. & BURLEY, S.D. (2015) Complex rift geometries resulting from inheritance of pre-existing structures: Insights and regional implications from the Barmer Basin rift. *J. Struct. Geol.*, 71, 136–154.
- BONINI, M., SOURIOT, T., BOCCALETTI, M. & BRUN, J.P. (1997) Successive orthogonal and oblique extension episodes in a rift zone: laboratory experiments with application to the Ethiopian Rift. *Tectonics*, 16(2), 347–362.
- CHATTOPADHYAY, A. & CHAKRA, M. (2013) Influence of preexisting pervasive fabrics on fault patterns during orthogonal and oblique rifting: an experimental approach. *Mar. Pet. Geol.*, 39, 74–91.
- CHENET, A.-L., GUIDELLEUR, X., FLUTEAU, F., COURTILLOT, V. & BAJPAI, S. (2007) 40K–40Ar dating of the Main Deccan large igneous province: further evidence of KTB age and short duration. *Earth Planet. Sci. Lett.*, 263, 1–15.
- CHOWDHARY, L.R. (1975) Reversal of basement-block motions in Cambay Basin, India, and its importance in petroleum exploration. *Am. Assoc. Pet. Geol. Bull.*, 59(1), 85–96.
- COLLIER, J.S., SANSOM, V., ISHIZUKA, O., TAYLOR, R.N., MINSHULL, T.A. & WHITMARSH, R.B. (2008) Age of Seychelles-India break-up. *Earth Planet. Sci. Lett.*, 272, 264–277.
- COMPTON, P.M. (2009) The geology of the Barmer Basin, Rajasthan, India, and the origins of its major oil reservoir, the Fatehgarh Formation. *Pet. Geosci.*, 15, 117–130.
- DANIELS, J.M. (2003) Floodplain aggradation and pedogenesis in a semiarid environment. *Geomorphology*, 56, 225–242.
- DOLSON, J., BURLEY, S.D., SUNDER, V.R., KOTHARI, V., NAIDU, B., WHITELEY, N.P., FARIMOND, P., TAYLOR, A., DIREEN, N. & ANANTHAKRISHNAN, B. (2015) The discovery of the Barmer Basin, Rajasthan, India, and its petroleum geology. *Am. Assoc. Pet. Geol. Bull.*, 99, 433–465.
- F€URISCH, F.T. & PANDEY, D.K. (2003) Sequence stratigraphic significance of sedimentary cycles and shell concentrations in the Upper Jurassic-Lower Cretaceous of Kachchh, Western India. *Palaeogeogr. Palaeoclimatol. Palaeoecol.*, 193, 285–309.
- GIBA, M., WALSH, J.J. & NICOL, A. (2012) Segmentation and growth of an obliquely reactivated normal fault. *J. Struct. Geol.*, 39, 253–267.
- GOMBOS, A.M. Jr, POWELL, W.G. & NORTON, I.O. (1995) The tectonic evolution of western India and its impact on hydrocarbon occurrences: an overview. *Sed. Geol.*, 96, 119–129.
- HENZA, A.A., WITHJACK, M.O. & SCHLISCHE, R.W. (2010) Normal-fault development during two phases of non-coaxial extension: an experimental study. *J. Struct. Geol.*, 32, 1656–1667.
- HENZA, A.A., WITHJACK, M.O. & SCHLISCHE, R.W. (2011) How do the properties of a pre-existing normal fault population

influence fault development during a subsequent phase of extension? *J. Struct. Geol.*, 33, 1312–1324.

HESTHAMMER, J. & FOSSEN, H. (1999) Evolution and geometries of gravitational collapse structures with examples from the Statfjord Field, northern North Sea. *Mar. Pet. Geol.*, 16, 259–281.

JAITLEY, A.K. & AJANE, R. (2013) Comments on *Placenticerias* Minto (Vredenburg, 1906) from the Bagh Beds (Late Cretaceous), Central India with Special Reference to Turonian Nodular Limestone Horizon. *J. Geol. Soc. India*, 81, 565–574.

KEEP, M. & MCCLAY, K.R. (1997) Analogue modelling of multiphase rift systems. *Tectonophysics*, 273, 239–270.

KHOSLA, A., KAPUR, V.V., SERENO, P.C., WILSON, J.A., WILSON, G.P., DUTHEIL, D., SAHNI, A., SINGH, M.P., KUMAR, S. & RANA, R.S. (2003) First Dinosaur remains from the Cenomanian-Turonian Nimar Sandstone (Bagh Beds), District Dhar, Madhya Pradesh, India. *J. Palaeontol. Soc. India*, 48, 115–127.

KRISHNA, J. (1987) An overview of the Mesozoic stratigraphy of Kachchh and Jaisalmer basins. *J. Palaeontol. Soc. India*, 32, 136–149.

LEZZAR, K.E., TIERCELIN, J.-J., Le TURDU, C., COHEN, A.S., REYNOLDS, D.J., Le GALL, B. & SCHOLZ, C.A. (2002) Control of normal fault interaction on the distribution of major Neogene sedimentary depocentres, Lake Tanganyika, East African rift. *Am. Assoc. Pet. Geol. Bull.*, 86(6), 1027–1059.

MAMTANI, M.A., KARANTH, R.V., MERH, S.S. & GREILING, R.O. (2000) Tectonic evolution of the southern part of Aravalli Mountain belt and its environs: possible causes and time constraints. *Gondwana Res.*, 3(2), 175–187.

MCCLAY, K. & KHALIL, S. (1998) Extensional hard linkages, eastern Gulf of Suez, Egypt. *Geology*, 26(6), 563–566.

MCCLAY, K.R., DOOLEY, T., WHITEHOUSE, P. & MILLS, M. (2002) 4-D evolution of rift-systems: insights from scaled physical models. *Am. Assoc. Pet. Geol. Bull.*, 86(6), 935–959.

MORGAN, W.J. (1971) Convection plumes in the lower mantle. *Nature*, 230, 42–43.

MORLEY, C.K. (1995) Developments in the structural geology of rifts over the last decade and their implications on hydrocarbon exploration. In: *Hydrocarbon Habitat in Rift Basins* (Ed. by J.J. Lambiase), pp. 1–32. Geological Society, London, Special Publications, 80.

MORLEY, C.K. (1999) How successful are analogue models in addressing the influence of pre-existing fabrics on rift structure? *J. Struct. Geol.*, 21, 1267–1274.

MORLEY, C.K., HARANYA, C., PHOOSONGSEE, W., PONGWAPEE, S., KORNSAWAN, A. & WONGANAN, N. (2004) Activation of rift oblique and rift parallel pre-existing fabrics during extension and their effect on deformation style: examples from the rifts of Thailand. *J. Struct. Geol.*, 26, 1803–1829.

MORLEY, C.K., GABDI, S. & SEUSUTTHIYA, K. (2007) Fault superimposition and linkage resulting from stress changes during rifting: examples from 3D seismic data, Phitsanulok Basin, Thailand. *J. Struct. Geol.*, 29, 646–663.

NIETO-SAMANIEGO, A.F. & ALANIZ-ALVAREZ, S.A. (1997) Origin and tectonic interpretation of multiple fault patterns. *Tectonophysics*, 270, 197–206.

PANDEY, D.K., F€EURISCH, F.T. & SHA, J.G. (2009) Interbasinal marker intervals – a case study from the Jurassic basins of Kachchh and Jaisalmer, western India. *Sci. China, Ser. D Earth Sci.*, 52(12), 1924–1931, doi: 10.1007/s11430-009-0158-0.

PANDEY, D.K., CHOUDHARY, S., BAHADUR, T., SWAMI, N., POONIA, D. & SHA, J. (2012) A review of the Lower – lowermost Upper Jurassic facies and stratigraphy of the Jaisalmer Basin, western Rajasthan, India. *Volumina Jurassica*, 10, 61–82.

PAREEK, H.S. (1981) Petrochemistry and Petrogenesis of the Malani Igneous Suite, India. *Geol. Soc. Am. Bull.*, 92(2), 206–273.

PLUMMER, P.S. & BELLE, E.R. (1995) Mesozoic tectono-stratigraphic evolution of the Seychelles microcontinent. *Sed. Geol.*, 96, 73–91.

RAI, J., SINGH, A. & PANDEY, D.K. (2013) Early to middle Albian age calcareous nannofossils from Pariwar Formation of Jaisalmer Basin, Rajasthan, western India and their significance. *Curr. Sci.*, 105(11), 1604–1611.

RAJU, A.T.R. (1968) Geological evolution of Assam and Cambay Tertiary Basins of India. *Am. Assoc. Pet. Geol. Bull.*, 52(2), 2422–2437.

REEVE, M.T., BELL, R.E. & JACKSON, C.A.-L. (2014) Origin and significance of intra-basement seismic reflections offshore western Norway. *J. Geol. Soc.*, 171, 1–4.

REEVES, C. (2013) The position of Madagascar within Gondwana and its movements during Gondwana dispersal. *J. Afr. Earth Sci.*, doi: 10.1016/j.afrearsci.2013.07.011.

ROHRMAN, M. (2007) Prospectivity of volcanic basins: trap delineation and acreage de-risking. *Am. Assoc. Pet. Geol. Bull.*, 91(6), 915–939.

ROY, A.B. (2003) Geological and geophysical manifestations of the R Eunion Plume-Indian lithosphere interactions – evidence from Northwest India. *Gondwana Res.*, 6(3), 487–500.

ROY, A.B. & JAKHAR, S.R. (2002) *Geology of Rajasthan (Northwest India): Precambrian to Recent*, p. 421. Scientific Publishers (India), Jodhpur.

SEN, A., PANDE, K., HEGNER, E., SHARMA, K.K., DAYAL, A.M., SHETH, H.C. & MISTRY, H. (2012) Deccan volcanism in Rajasthan: ⁴⁰Ar-³⁹Ar geochronology and geochemistry of the Tavidar volcanic suite. *J. Asian Earth Sci.*, 59, 127–140.

SHARMA, K.K. (2007) K-T magmatism and basin tectonism in western Rajasthan, India: results from external tectonics and not from R Eunion plume activity. In: *Plates, Plumes and Planetary Processes* (Ed. by G.R. Foulger & D.M. Jurdy), pp. 775–784. Geological Society of America Special Paper, 430, doi: 10.1130/2007.2430(35).

SHETH, H.C. (2005a) Were the Deccan flood Basalts derived in part from ancient oceanic crust within the Indian continental lithosphere? *Gondwana Res.*, 8(2), 109–127.

SHETH, H.C. (2005b) From Deccan to R Eunion: no trace of a mantle plume. In: *Plates, Plumes and Paradigms* (Ed. by G.R. Foulger, J.H. Natland, D.C. Presnall & D.L. Anderson), pp.

477–501. Geological Society of America Special Paper, 388, doi: 10.1130/2005.2388(29).

SHETH, H.C. (2007) Plume-related regional prevolcanic uplift in the Deccan Traps: absence of evidence, evidence of absence. In: *Plates, Plumes and Planetary Processes* (Ed. by G.R. Foulger & D.M. Jurdy), pp. 785–813. Geological Society of America Special Paper, 430, doi: 10.1130/2007.2430(36).

SIMONETTI, A., BELL, K. & VILADKAR, S.G. (1995) Isotopic data from the Amba Dongar carbonatite complex, west–central India: evidence for an enriched mantle source. *Chem. Geol.*, 122, 185–198.

SIMONETTI, A., GOLDSTEIN, S.L., SCHMIDBERGER, S.S. & VILADKAR, S.G. (1998) Geochemical and Nd, Pb, and Sr isotope data from deccan alkaline complexes–inferences for mantle sources and plume–lithosphere interaction. *J. Petrol.*, 39, 1847–1864.

SINGH, N.P. (2006) Mesozoic lithostratigraphy of the Jaisalmer Basin, Rajasthan. *J. Palaeontol. Soc. India*, 51(2), 1–25.

SINGH, N.P. (2007) Cenozoic lithostratigraphy of the Jaisalmer Basin, Rajasthan. *J. Palaeontol. Soc. India*, 52(2), 129–154.

SISODIA, M.S. & SINGH, U.K. (2000) Depositional environment and hydrocarbon prospects of the Barmer Basin, Rajasthan, India. *Nafta, Zagreb (Croatia)*, 51(9), 309–326.

STOREY, M., MAHONEY, J.J., SAUNDERS, A.D., DUNCAN, R.A., KELLEY, S.P. & COFFIN, M.F. (1995) Timing of hot spot related volcanism and the breakup of Madagascar and India. *Science*, 267, 852–855.

TORSVIK, T.H., PANDIT, M.K., REDFIELD, T.F., ASHWAL, L.D. & WEBB, S.J. (2005) Remagnetization of Mesozoic limestones from the Jaisalmer basin, NW India. *Geophys. J. Int.*, 161, 57–64.

VIJAYA RAO, V., RAJENDRA PRASAD, B., REDDY, P.R. & TEWARI, H.C. (2000) Evolution of Proterozoic Aravalli Delhi fold belt in the northwestern Indian shield from seismic studies. *Tectonophysics*, 327, 109–130.

WHIPP, P.S., JACKSON, C.A.-L., GAWTHORPE, R.L., DREYER, T. & QUINN, D. (2014) Fault array evolution above a reactivated rift-fabric; a subsurface example from the northern Horda Platform fault array, Norwegian North Sea. *Basin Res.*, doi: 10.1111/bre.12050.

WILLEMSE, E.J.M. (1997) Segmented normal faults: correspondence between three-dimensional mechanical models and field data. *J. Geophys. Res.*, 102(B1), 675–692.

YOUNES, A.I. & MCCLAY, K. (2002) Development of accommodation zones in the Gulf of Suez – Red Sea rift, Egypt. *Am. Assoc. Pet. Geol. Bull.*, 86(6), 1003–1026.

FIGURES

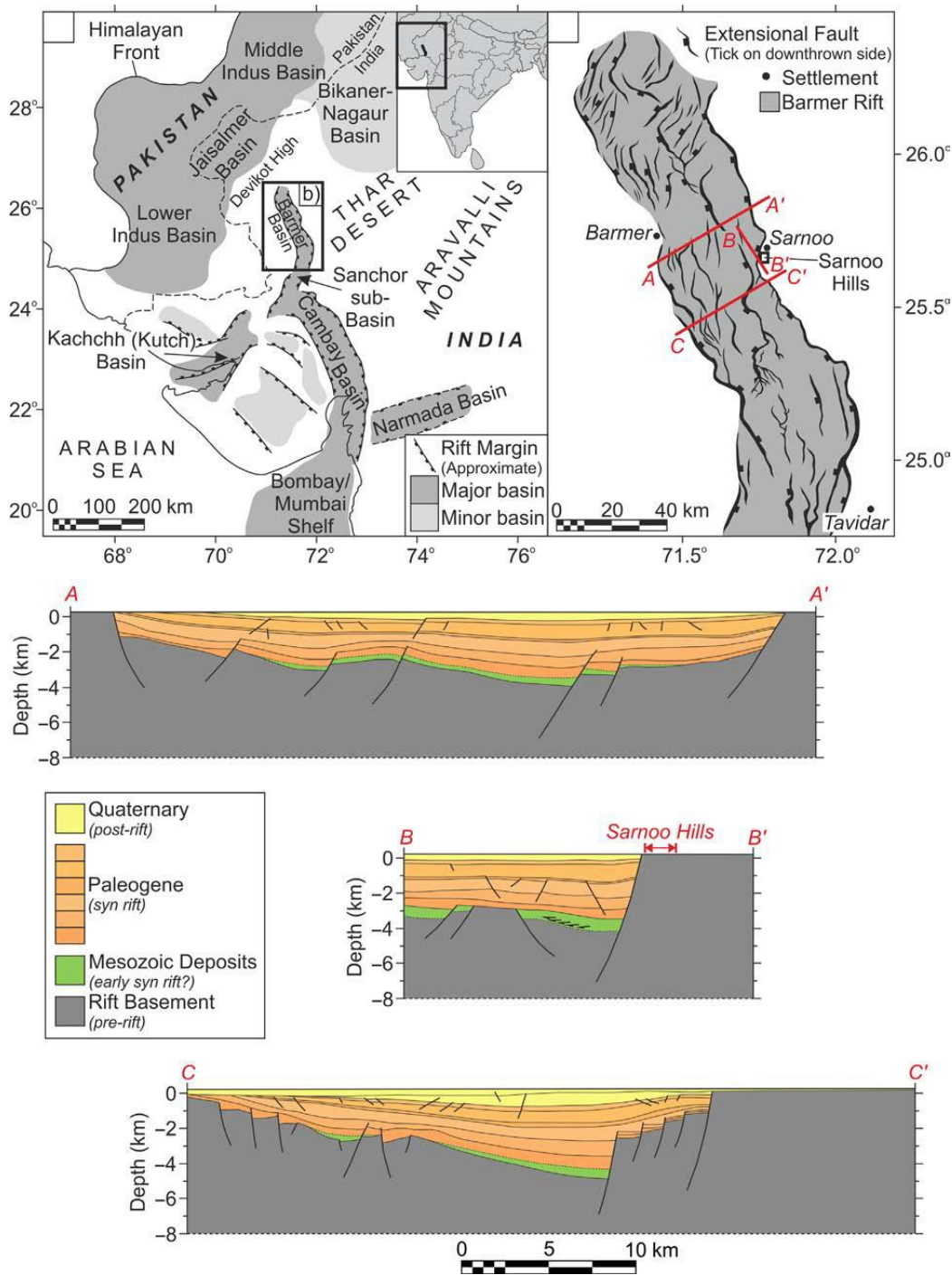


Fig. 1. (a) Onshore rift basins of northwest India; (b) Structure map of the Barmer Basin at the pre-rift unconformity horizon. The location of the Sarnoo Hills is indicated; (c–e) interpreted seismic sections across the central Barmer Basin in the vicinity of the Sarnoo Hills. See (b) for section locations.

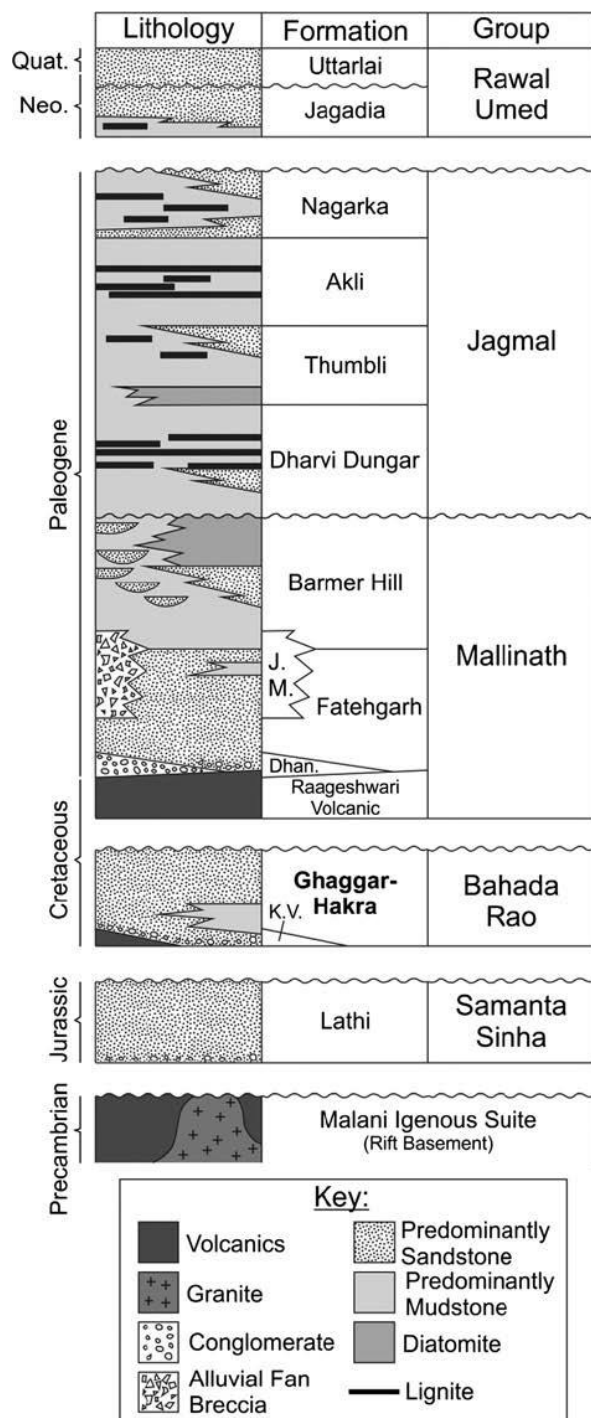


Fig. 2. Barmer Basin generalised vertical section. Stratigraphy relevant to this work, the Ghaggar-Hakra Formation, is highlighted in bold. K.V. = Karentia Volcanic; Dhan. = Dhandlawas; J.M. = Jogmaya Mandir; Neo. = Neogene; Quat. = Quaternary.

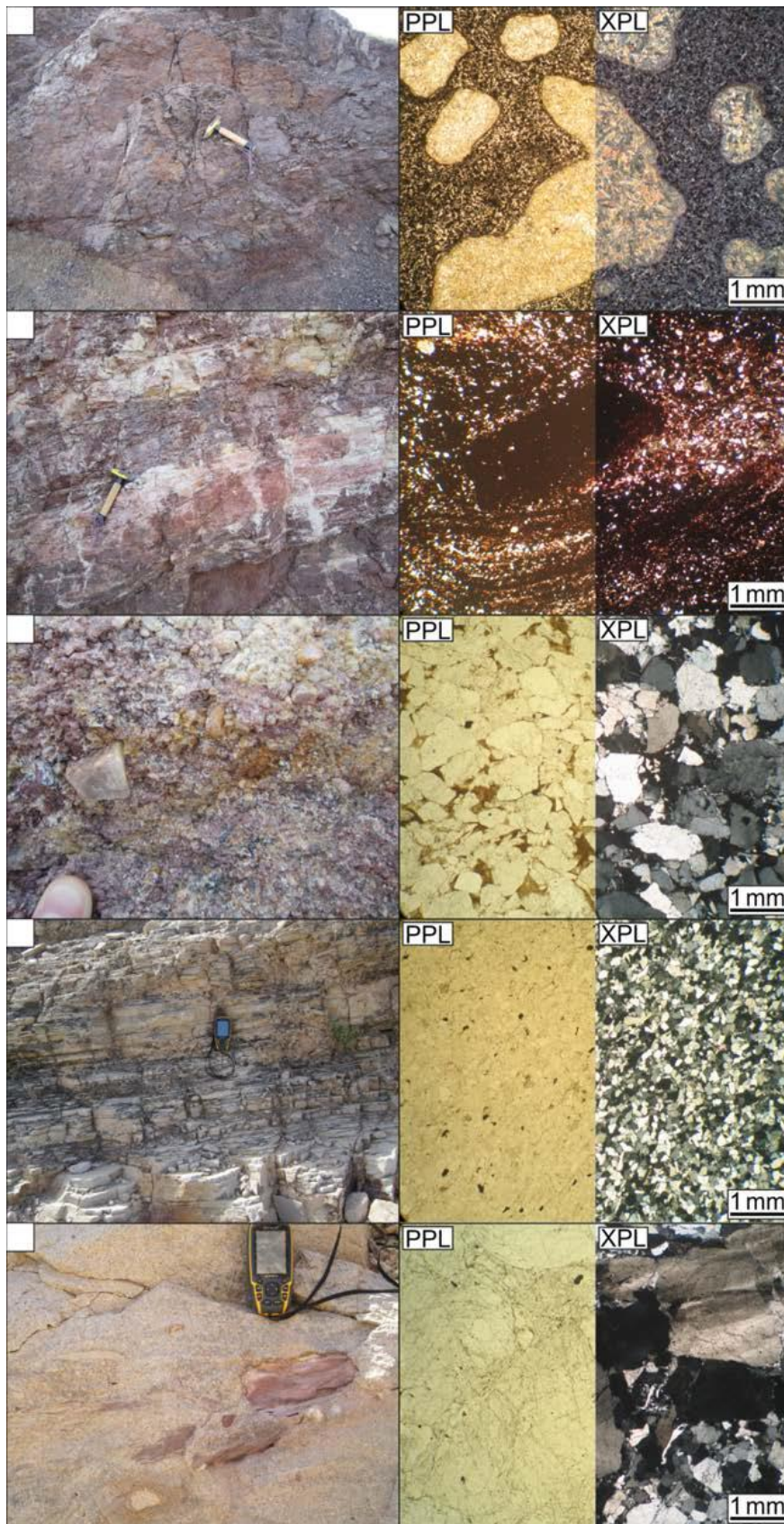


Fig. 3. Outcrop (left) and thin section (right) images of each mapping unit exposed in the Sarnoo Hills: (a) basalt at the base of the succession; (b) siltstone packages of the Ghaggar-Hakra Formation (gha); (c) the Darjaniyon-ki Dhani Sandstone (dar); (d) the Sarnoo Sandstone (sar); (e) the Nosar Sandstone (nos).

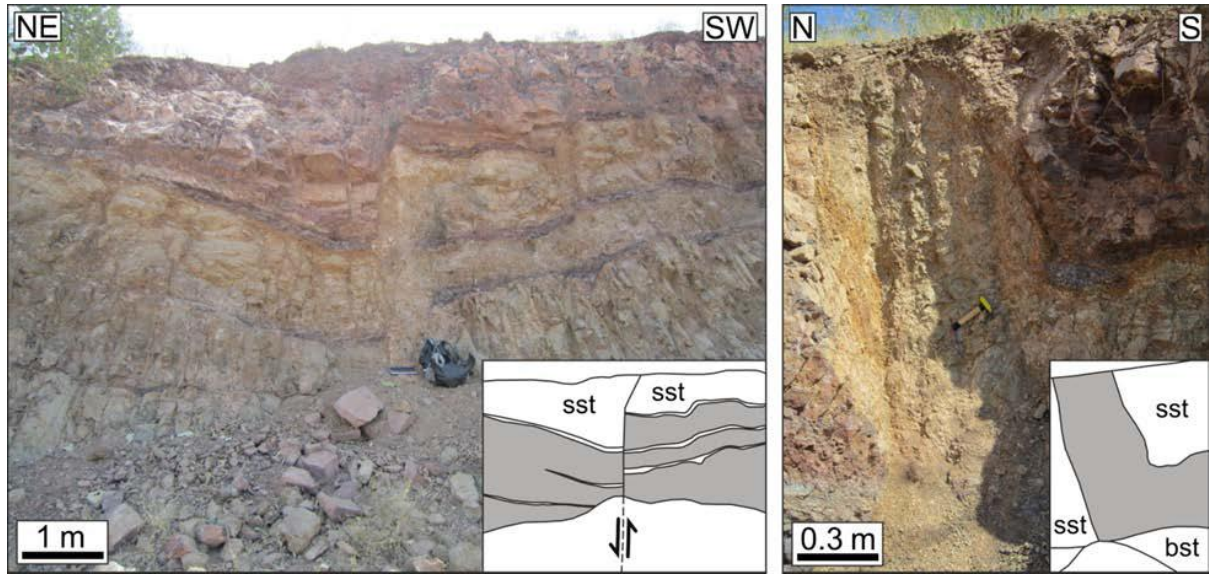


Fig. 4. A heavily altered, poorly consolidated, light green crystalline unit is exposed towards the base of the sedimentary succession, and appears both interbedded (a) [GR 0779583 2841933 UTM zone 42N] and to intrude into (b) [GR 0779992 2842124 UTM zone 42N], the lowermost Ghaggar-Hakra Formation. Photos were taken from Darjaniyon-ki Dhani Hill, approximately 500 m east of the north Sarnoo Hills. Sketch interpretations of each photograph are inset; grey = heavily altered, poorly consolidated, light green crystalline unit; sst = sandstone; bst = basalt.

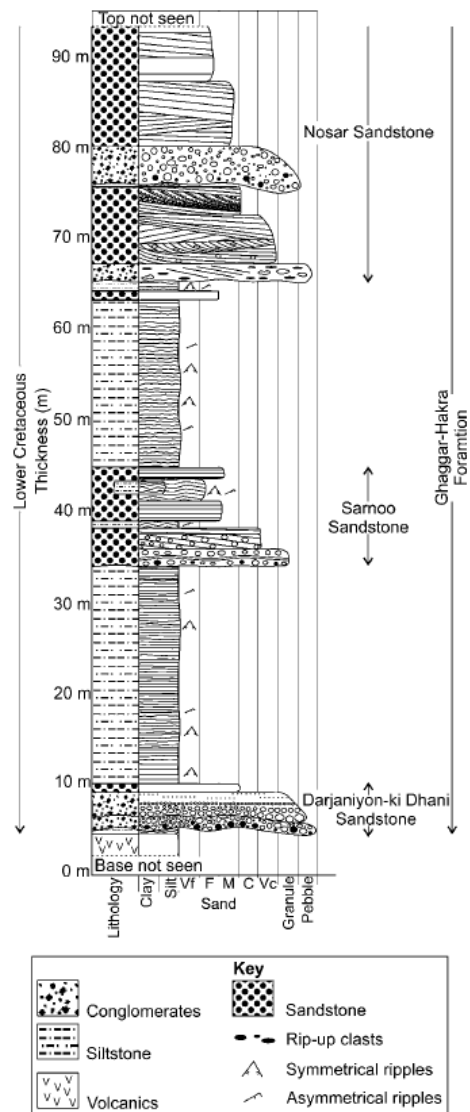


Fig. 5. Generalised sedimentary log through the Lower Cretaceous Ghaggar-Hakra Formation, comprising three sandstone successions, the Nosar Sandstone, Sarnoo Sandstone, and Darjaniyon-ki Dhani Sandstone, interbedded with thick packages of siltstone. Vf = Very fine; F = Fine; M = Medium; C = Coarse; Vc = Very coarse.

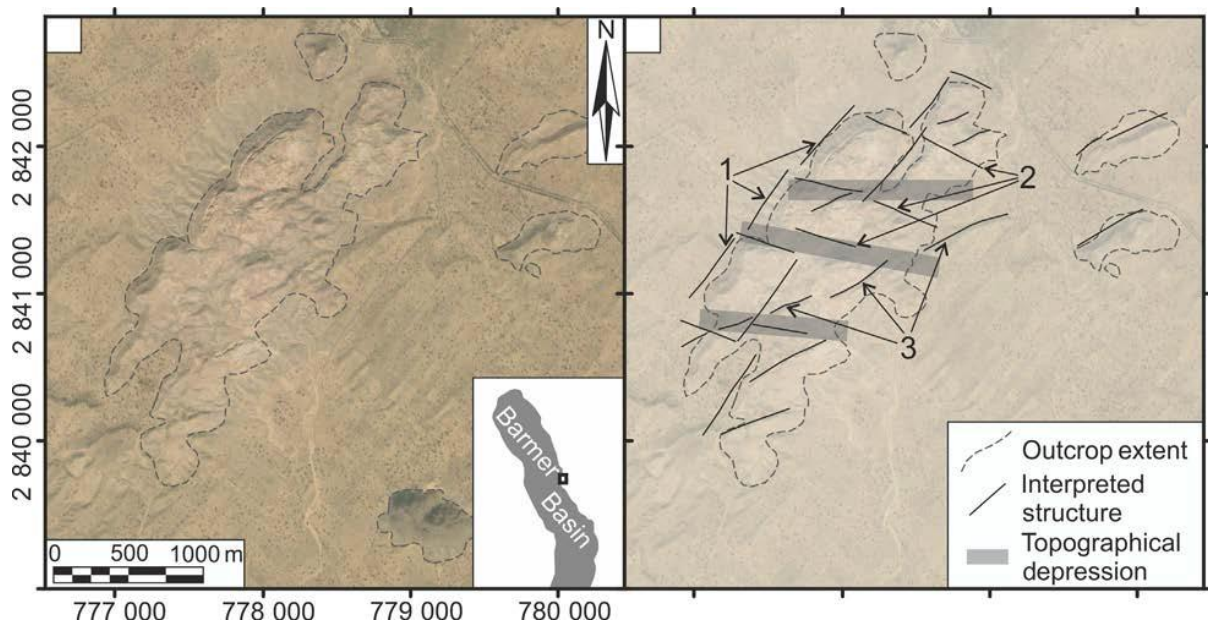


Fig. 6. (a) Satellite image of exposure at the Sarnoo Hills (location map inset). Image courtesy of GoogleTM earth. The limit of the exposure is dashed; (b) Interpretation of (a) indicating three main structural trends (1, 2 & 3). Three prominent outcrop-dissecting topographical depressions are also indicated (key inset).

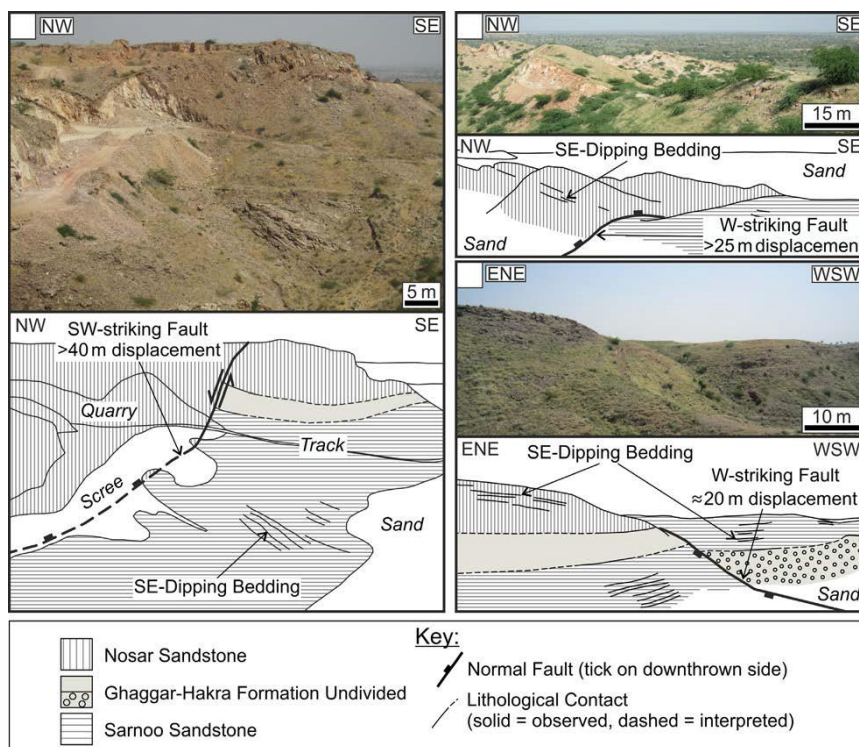


Fig. 7. Juxtaposition of the distinct sandstone successions within the Ghaggar-Hakra Formation indicates the location of major SWstriking, NW-dipping (a) and W-striking, N-dipping (b, c) faults in the Sarnoo Hills. For image locations see Fig. 8.

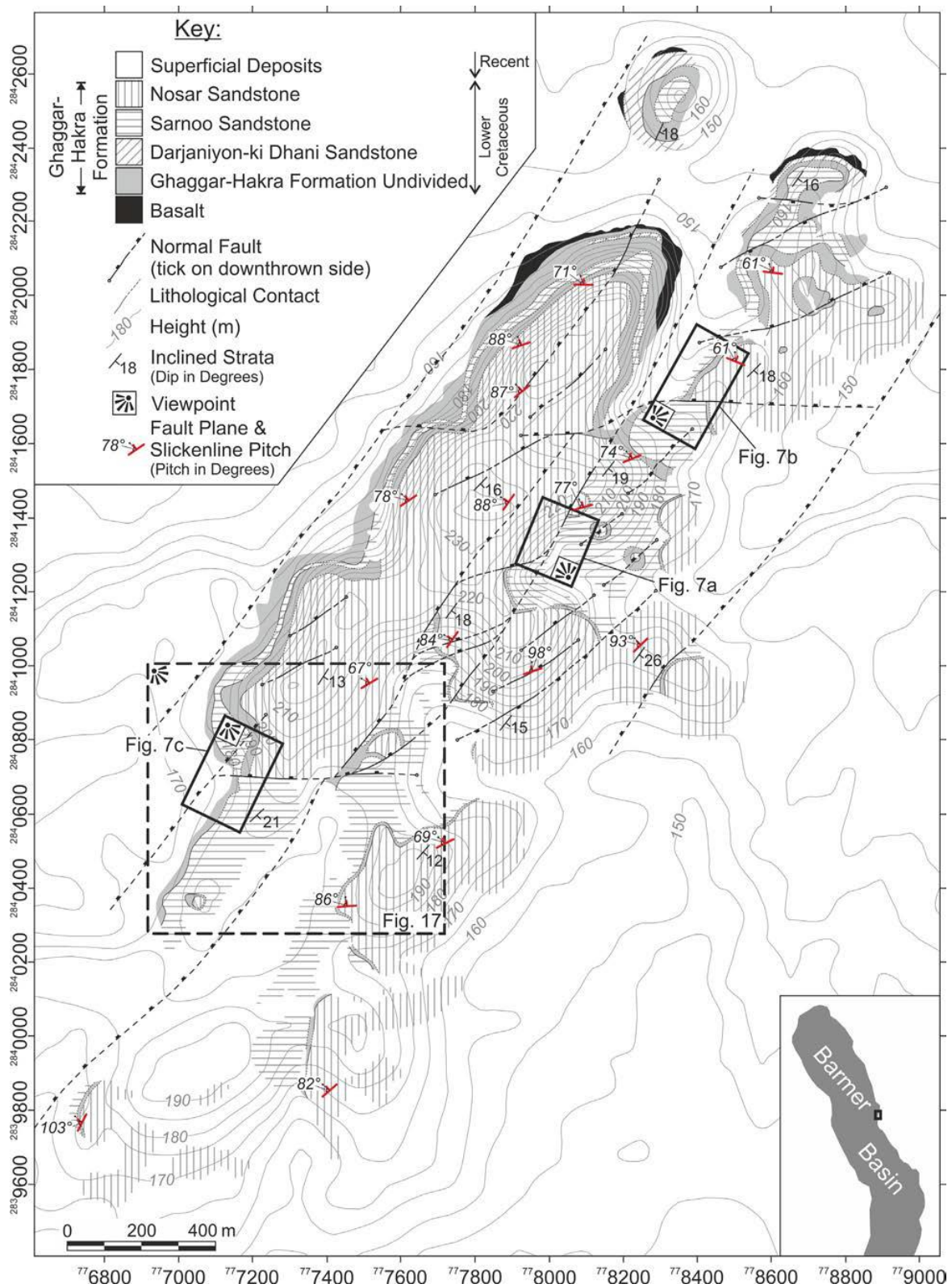


Fig. 8. The Samoo Hills, east Barmer rift (location map and key inset). Topographical contours are at 5 m intervals. Reference grid is UTM zone 42N. The locations and viewpoints of Figs 7 and 17 are indicated. Fault slip data for selected (often minor) faults are also shown.

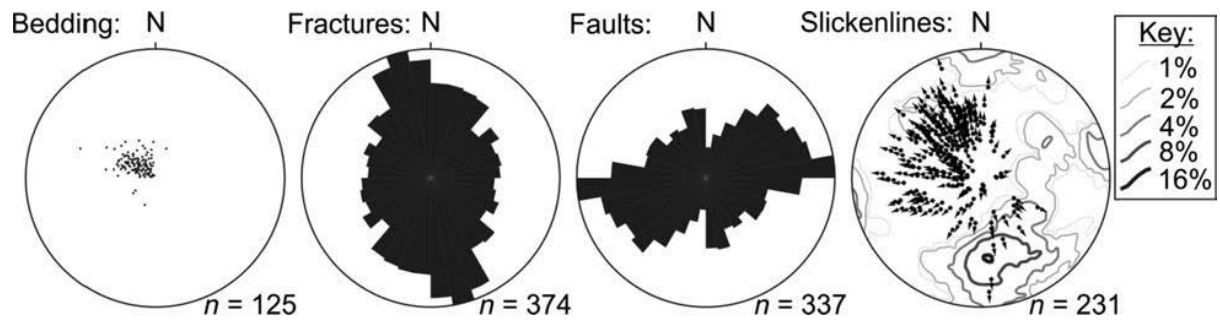


Fig. 9. Structural data from the Sarnoo Hills, indicating a gentle stratigraphical dip to the southeast, a predominance of north-northwest-trending fractures and west-trending faults, and fault slip to the northwest. Contours on slickenline plot represent density of poles-to-fault plane measurements by area (key inset). All stereographic projections are lower hemisphere, equal area. Rose diagrams are equal area.

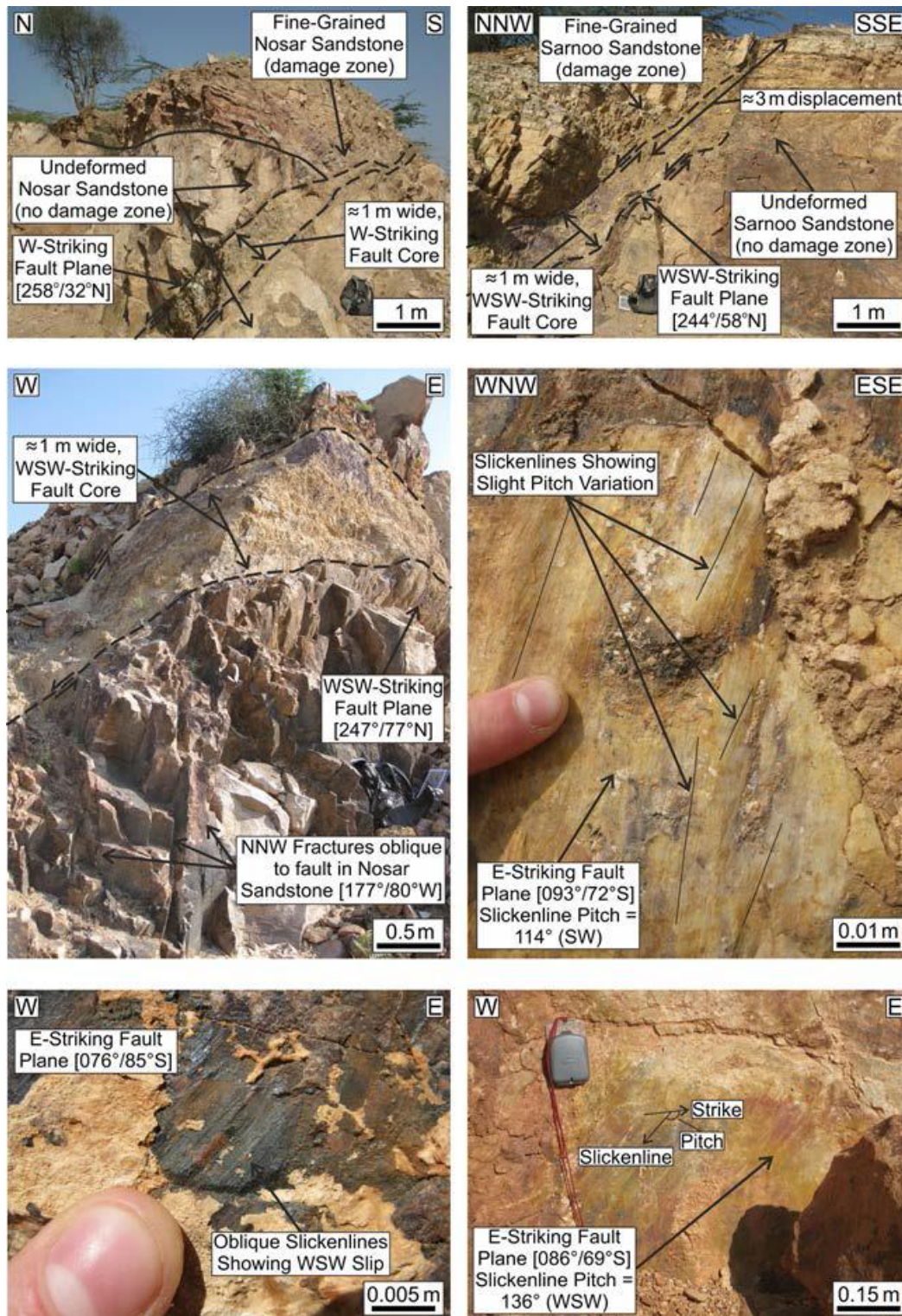


Fig. 10. Structures exposed in the Sarnoo Hills. Fault measurements are recorded as strike/dip/sense and pitch-in-plane is measured from fault strike, with the general lineation trend shown in brackets. (a) Southwest-striking fault within the Nosar Sandstone. GR 0778854 2841939 UTM zone 42N; (b) West-southwest-striking fault within the Sarnoo Sandstone. GR 0778297 2842497 UTM zone 42N; (c) north-northwest-trending fractures abutting obliquely against a southwest-striking fault. GR 0777724 2841071 UTM zone 42N; (d) Multiple slickenline sets on an exposed fault plane. GR 0778003 2841662 UTM zone 42N; (e) Slickenlines displaying highly oblique slip towards the west-southwest. GR 0778081 2841838 UTM zone 42N; (f) Slickenlines exposed on an east-striking fault displaying dextral-oblique slip towards the west-southwest. GR 0777807 2841045 UTM zone 42N.

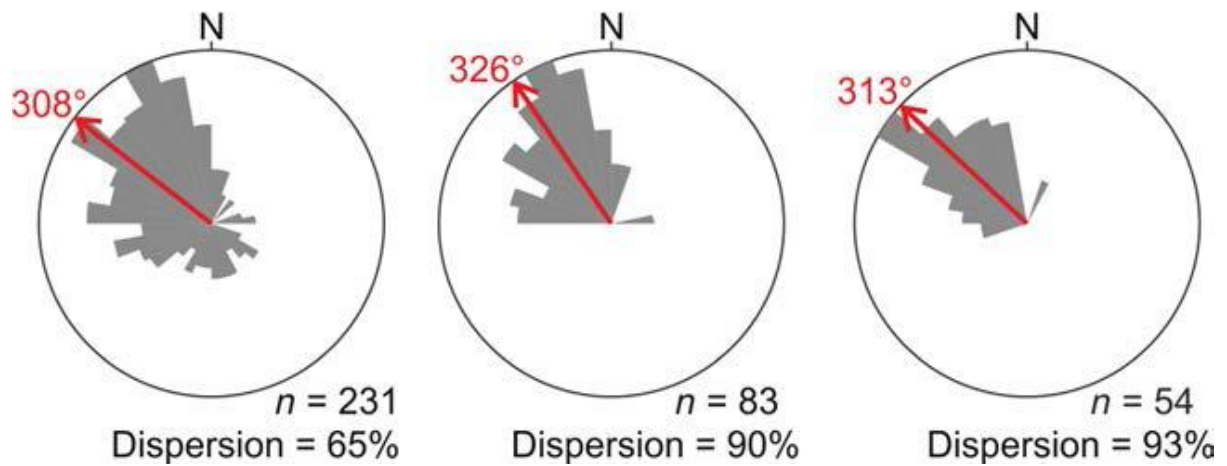


Fig. 11. Fault slip data from the Sarnoo Hills. The azimuth of the vector mean (arrowed) and dispersion are shown for each data set. All rose plots are equal area. (a) all Sarnoo slickenlines; (b) slickenlines measured on west-striking (247.5° – 292.5°) faults; (c) slickenlines measured on southwest-striking (202.5° – 247.5°) faults.

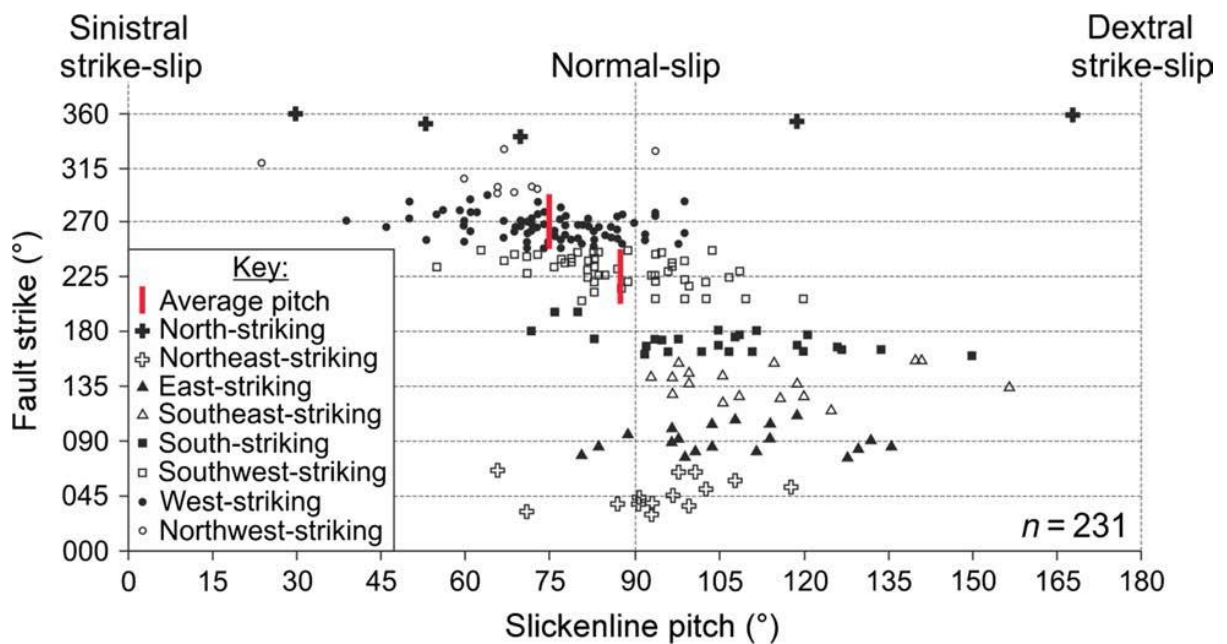


Fig. 12. Slickenline pitch vs. fault strike plot. Average fault slip on SW-striking, NW-dipping faults displays a 3° component of sinistral-oblique slip (average pitch = 87°). In contrast, average W-striking, N-dipping faults display a significantly larger (15°) component of sinistral-oblique slip (average pitch = 75°).

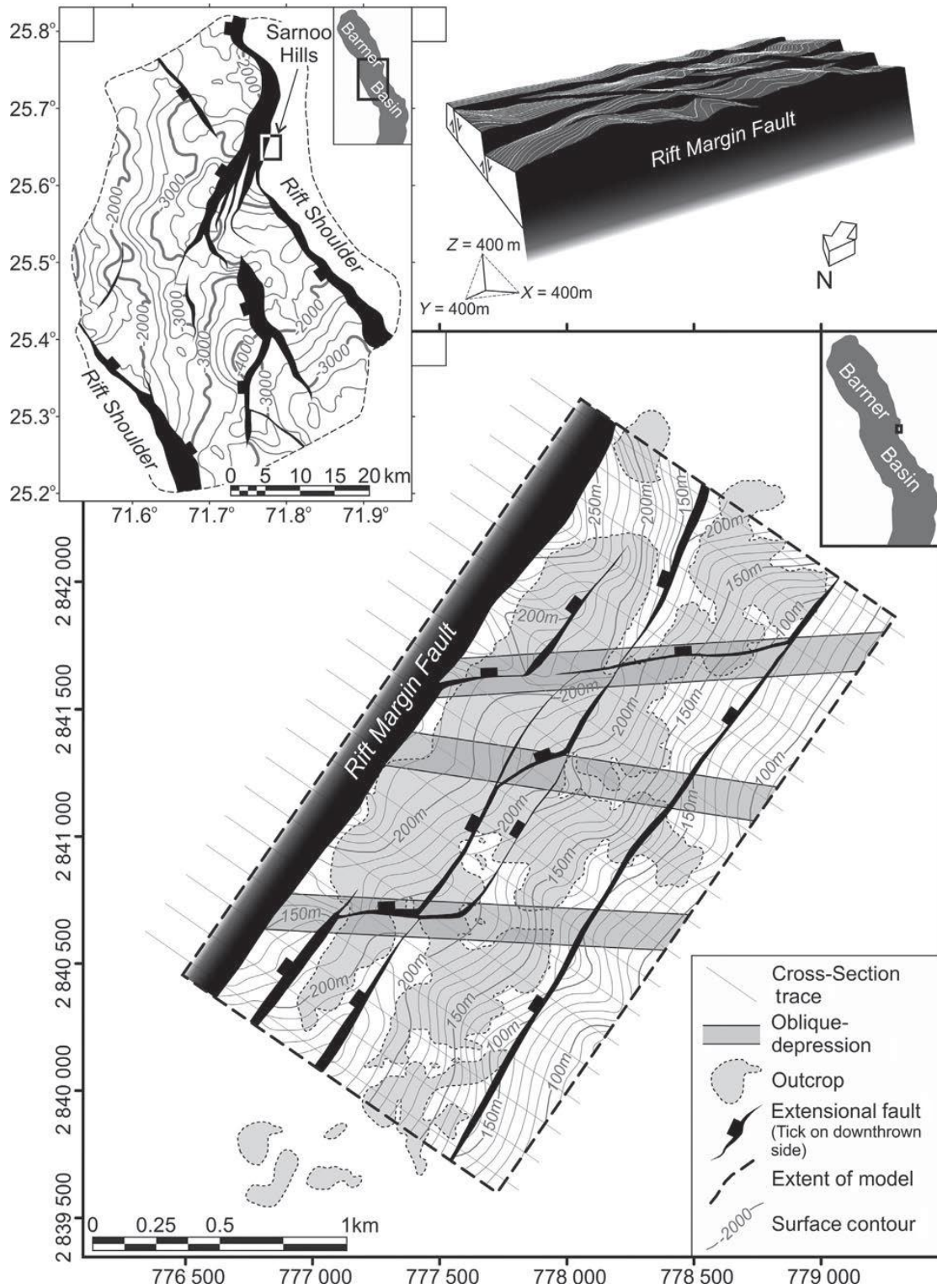


Fig. 13. (a) Time-structure map of the pre-rift unconformity in the central Barmer Basin rift. The location of the Sarnoo Hills is indicated; (b) three-dimensional view of the base Nosar Sandstone surface, taken from the virtual model of the outcrop; (c) contoured base Nosar Sandstone surface from the virtual model of the outcrop. Fault polygons from the base Nosar Sandstone surface are overlain. Contours are of elevation in metres (location within the Barmer Basin inset) and cross-section traces from which the model was constructed are also displayed.

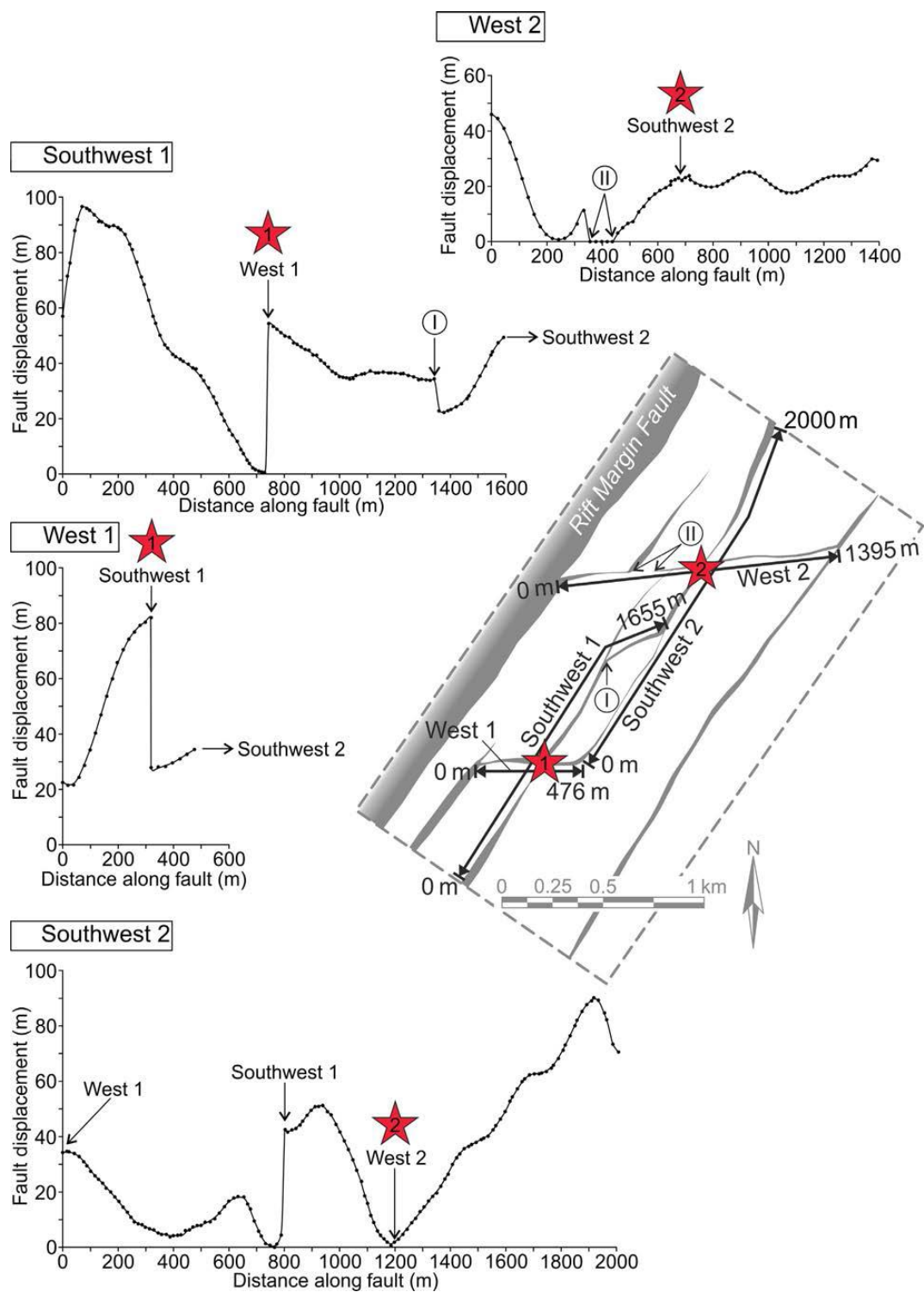


Fig. 14. Fault displacement-length profiles constructed from the base Nosar Sandstone surface in the virtual outcrop model. Displacement measurements were taken at 10–20 m intervals. Stars indicate where a reactivated fault segment restricted the evolution of an extension-perpendicular fault.

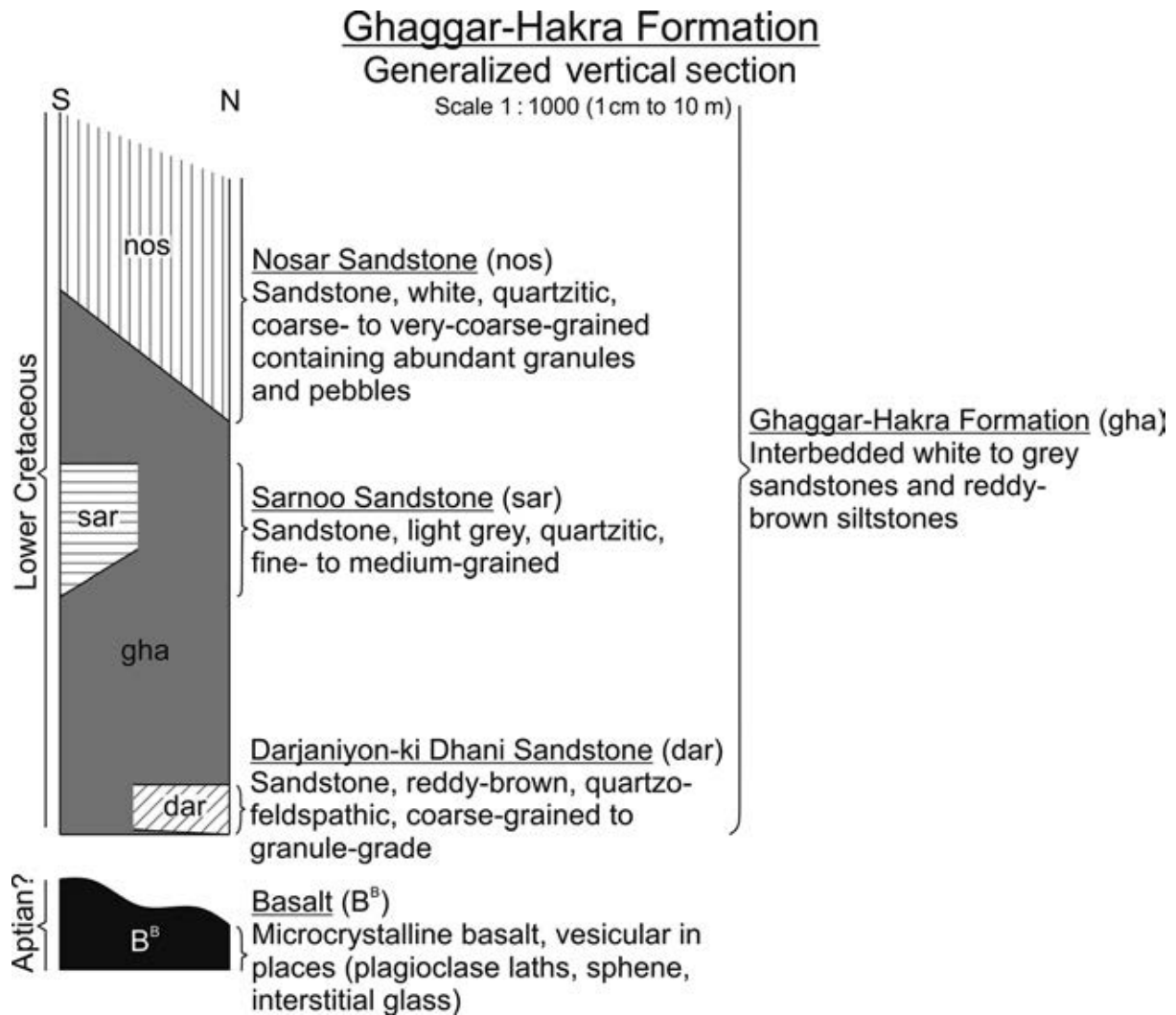


Fig. 15. Generalised vertical section depicting the spatial relationship of mapping units within the Lower Cretaceous Ghaggar-Hakra Formation sedimentary succession, as exposed in the Sarnoo Hills area, east Barmer Basin. Three channelised fluvial sandstone successions (dar; sar; nos) are separated by a thick (< 50 m) package of mudstones and siltstones (gha) representing the floodplain environment that accompanied the fluvial systems. The high proportion of fine deposits within the succession suggests floodplain aggradation, possibly due to rapid subsidence and a high sediment supply.

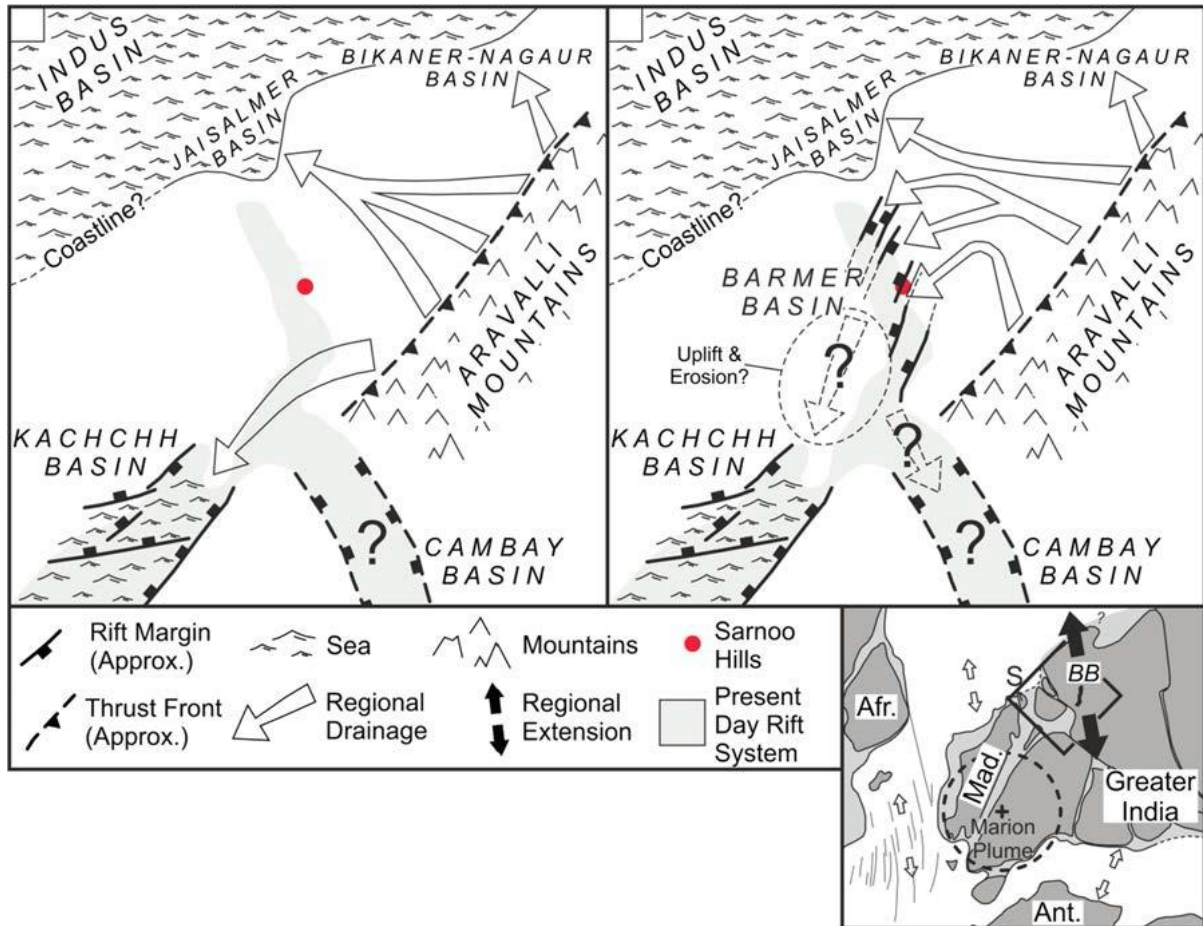


Fig. 16. Paleogeography cartoons of northwest India (a) tectonic quiescence in the Barmer region prior to the onset of NW–SE extension; (b) the onset of NW–SE extension induced SW-trending faulting in the Barmer region, and may have captured established regional drainage systems within early rift-oblique (northeast–southwest) rift systems. Afr = Africa, S = Seychelles microcontinent, Mad. = Madagascar, BB = Barmer Basin, Ant. = Antarctica. Plate reconstruction at 120 Ma inset (redrawn from Reeves 2013).

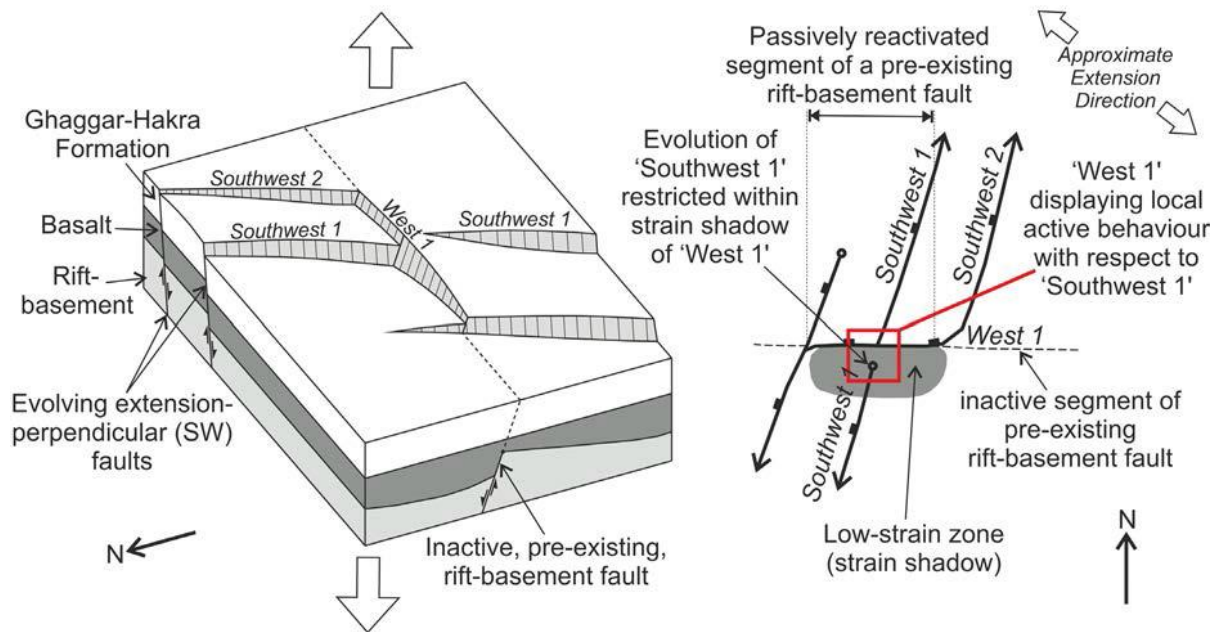


Fig. 17. In the Sarnoo Hills, passively reactivated segments of pre-existing rift-basement faults restricted the evolution of the evolving, extension-perpendicular faults, and locally displayed active behaviour. Light grey = Malani Igneous Suite rift basement; dark grey = basalt; white = Ghaggar-Hakra Formation; (a) Block diagram; (b) annotated sketch map of (a).